Horizon 2020 Programme

METIS

Research and Innovation Action (RIA)

This project has received funding from the European Union's Horizon 2020 research and innovation programme under grant agreement No 945121

Start date : 2020-09-01 Duration : 57 Months

Report on scalar and multi-dimensional (vector-based) fragility evaluation methods and implementation in opensource software

Authors : Mrs. Mohamed ZOUATINE (TUK)

METIS - Contract Number: 945121

Project officer: Katerina PTACKOVA

Document title	Report on scalar and multi-dimensional (vector-based) fragility evaluation methods and implementation in opensource software
Author(s)	Mrs. Mohamed ZOUATINE
Number of pages	51
Document type	Deliverable
Work Package	WP6
Document number	D6.5
Issued by	TUK
Date of completion	2025-04-23 11:31:51
Dissemination level	Public

Summary

This report provides a comprehensive evaluation of scalar and vector intensity measures (IMs) in fragility analysis, focusing on both linear and nonlinear structural responses. Using the Diesel Generator Building of the Zaporizhzhia Nuclear Power Plant (NPP) as a case study, a simplified model was developed and validated against a complex model. Fragility analyses were conducted using two primary methodologies: Cloud analysis, which employed unscaled ground motions, and Incremental Dynamic Analysis (IDA), which utilized scaled ground motions. These analyses incorporated two statistical approaches, Multiple Linear Regression (MLR) and Maximum Likelihood Estimation (MLH), with drift and acceleration as engineering demand parameters (EDPs). The scalar analysis evaluated the performance of IMs using three statistical parameters: dispersion (?), Akaike Information Criterion (AIC), and Area Under the Curve (AUC). The results consistently identified spectral acceleration at the fundamental period Sa(T1) as the most effective scalar IM in minimizing uncertainties for both considered responses. The vector-based analysis extended this evaluation by combining multiple IMs to further reduce dispersion and improve fragility predictions. Sa(T1) a critical component in optimal IM combinations, such as (Sa(T1), Np), which resulted in the lowest. The benefits of vector IMs were more pronounced in nonlinear responses, highlighting their potential to address structural behaviours that exhibit significant nonlinearity. Roof Drift as an EDP consistently yielded lower dispersion compared to roof acceleration, reinforcing its reliability for fragility assessments. This observation held true for both scalar and vector approaches. In conclusion, this report emphasizes the importance of selecting appropriate IMs and EDPs for fragility analysis. While scalar IMs, particularly Sa(T1), provide robust results, vector IMs demonstrate enhanced performance in reducing uncertainties, especially in nonlinear scenarios.

Approval

Date	By
2025-04-23 11:35:30	Mrs. Mohamed ZOUATINE (TUK)
2025-04-29 07:50:47	Dr. Irmela ZENTNER (EDF)

METIS

Seismic Risk Assessment for Nuclear Safety

Research & Innovation Action

NFRP-2019-2020

Report on scalar and multi-dimensional (vector based) fragility evaluation methods

Deliverable D6.5

Version N°1

Authors:

Mohamed Zouatine M.Sc (RPTU)

Prof. Dr.-Ing. Hamid Sadegh-Azar (RPTU)

Disclaimer

The content of this deliverable reflects only the author's view. The European Commission is not responsible for any use that may be made of the information it contains.

Document Information

Grant agreement	945121
Project title	Methods And Tools Innovations for Seismic Risk Assessment
Project acronym	METIS
Project coordinator	Dr. Irmela Zentner, EDF
Project duration	1st September 2020 – 31st May 2025 (57 months)
Related work package	WP 6 – Beyond Design and Fragility Analysis
Related task(s)	Task 6.5 – Report on scalar and multi-dimensional (vector based) fragility evaluation methods
Lead organisation	TUK
Contributing partner(s)	TUK
Due date	31st May 2024
Submission date	23/04/2025
Dissemination level	Public

History

Version	Submitted by	Reviewed by	Date	Comments
N°1	Mohamed Zouatine	Karaferis Nikolaos & Dimitrios Vamvatsikos	22/11/2024	
N°2	Mohamed Zouatine	Dmytro Ryzhov	26/03/2025	

Table of Contents

List of Figures

List of Tables

Abbreviations and Acronyms

Acronym	Description
NPP	Nuclear Power Plant
SSC	System, Structure, Component
FEM	Finite Element Model
MLR	Multiple Linear regression
MLH	Maximum Likelihood
DGB	Diesel Generator Building
AIC	Akaike information criterion
AUC	Area Under the Curve
LHS	Latin Hypercube Sampling
IM	Intensity Measure
PGA	Peak Ground Acceleration
EDP	Engineering Demand Parameter
BE	Best Estimate
BEU	Best Estimate and Uncertainties
V-IM	Vector Intensity Measure
IDA	Incremental Dynamic Analysis

Summary

This report provides a comprehensive evaluation of scalar and vector intensity measures (IMs) in fragility analysis, focusing on both linear and nonlinear structural responses. Using the Diesel Generator Building of the Zaporizhzhia Nuclear Power Plant (NPP) as a case study, a simplified model was developed and validated against a complex model. Fragility analyses were conducted using two primary methodologies: Cloud analysis, which employed unscaled ground motions, and Incremental Dynamic Analysis (IDA), which utilized scaled ground motions. These analyses incorporated two statistical approaches, Multiple Linear Regression (MLR) and Maximum Likelihood Estimation (MLH), with drift and acceleration as engineering demand parameters (EDPs).

The scalar analysis evaluated the performance of IMs using three statistical parameters: dispersion (β), Akaike Information Criterion (AIC), and Area Under the Curve (AUC). The results consistently identified spectral acceleration at the fundamental period Sa(T1) as the most effective scalar IM in minimizing uncertainties for both considered responses.

The vector-based analysis extended this evaluation by combining multiple IMs to further reduce dispersion and improve fragility predictions. Sa(T1) a critical component in optimal IM combinations, such as (Sa(T1), Np), which resulted in the lowest. The benefits of vector IMs were more pronounced in nonlinear responses, highlighting their potential to address structural behaviours that exhibit significant nonlinearity.

Roof Drift as an EDP consistently yielded lower dispersion compared to roof acceleration, reinforcing its reliability for fragility assessments. This observation held true for both scalar and vector approaches.

In conclusion, this report emphasizes the importance of selecting appropriate IMs and EDPs for fragility analysis. While scalar IMs, particularly Sa(T1), provide robust results, vector IMs demonstrate enhanced performance in reducing uncertainties, especially in nonlinear scenarios.

Keywords

Vector & scalar fragility, intensity measure, uncertainty propagation, Engineering Demand Parameter.

Introduction

The aim of Deliverable D6.5, titled "Report on Scalar and Multi-Dimensional (Vector-Based) Fragility Evaluation Methods," is to evaluate the effectiveness of different combinations of intensity measures (IMs)—both structural and ground-motion related—through scalar and vector-based fragility methodologies. This report aims to compare these methodologies, emphasizing the advantages of vector-based approaches in reducing uncertainties and improving the reliability of fragility assessments.

The analysis was conducted using a simplified model of the Diesel Generator Building at the Zaporizhzhia Nuclear Power Plant (NPP), validated against a more complex model. This model serves as the foundation for fragility evaluations, considering both linear and nonlinear structural responses. Two fragility methodologies were employed: Cloud analysis, which uses unscaled natural ground motions, and Incremental Dynamic Analysis (IDA), where ground motions are scaled to different intensity levels. Both approaches incorporated two statistical techniques—Multiple Linear Regression (MLR) and Maximum Likelihood Estimation (MLH)—to compute the fragility parameters, with drift and acceleration as the engineering demand parameters (EDPs).

The report is structured into four primary sections. Section 1 describes the ground motions utilized to construct the fragility curves for both scalar and vector intensity measures. Section 2 outlines the approach employed to develop a simplified model of a complex nuclear power structure, which serves as the case study for this analysis. Section 3 evaluates the performance of scalar intensity measures based on dispersion, while other statistical parameters are used to assess the quality of the fitting, comparing two distinct fragility methodologies: one without ground motion scaling (Cloud method) and another with ground motion scaling (Incremental Dynamic Analysis, IDA). This comprehensive comparison considers different phases of structural behaviour, both linear and nonlinear, and examines two engineering demand parameters (EDPs) to identify which provides a stronger correlation with various intensity measures (IMs). Additionally, two methodologies—regression and maximum likelihood estimation—are used to compute the parameters of the fragility curves. Section 4 follows a similar workflow, focusing instead on vector-based intensity measures.

1 Metis Case Study Site, and Ground Motion Record Selection

The numerical models developed within the Metis project to represent the Zaporizhzhia Nuclear Power Plant (NPP) were assumed to be located in Tuscany, Italy. Ground motions from Work Package 5 (WP5) were utilized to reflect the site-specific conditions accurately. These ground motions from WP5 are organized into ten distinct intensity measure levels (IMLs), each corresponding to a different return period. For the site response analysis, five of these IMLs (5, 6, 7, 8, and 9) were selected Table 1.1. In conducting the site response analysis, uncertainties were systematically accounted for. Consequently, the final results of WP5 are classified into two main categories: Best Estimate (BE) and Best Estimate with Uncertainties (BEU), representing ground motion at the surface level with and without consideration of uncertainties on site properties, respectively Fig 1.1.

Table 1.1 IML values for different return periods

IMLs	**5**	**6**	**7**	**8**	**9**
Return Period (yrs)	2500	5000	10000	20000	50000
IM*=PGA (g)	0.132	0.191	0.27	0.377	0.565

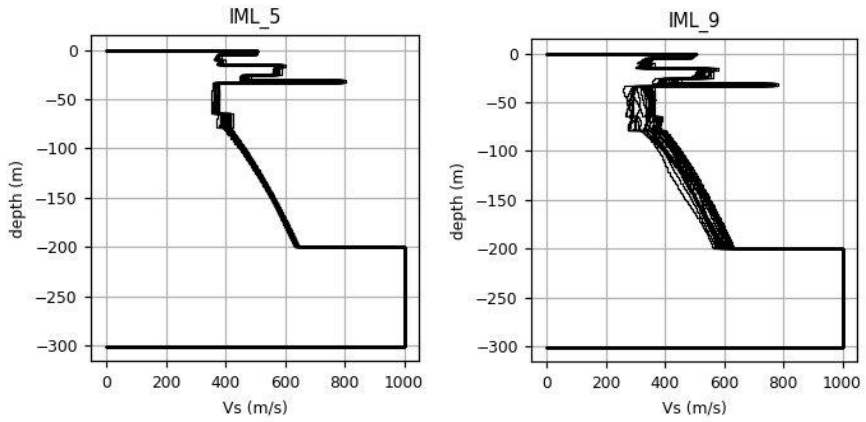

(a)

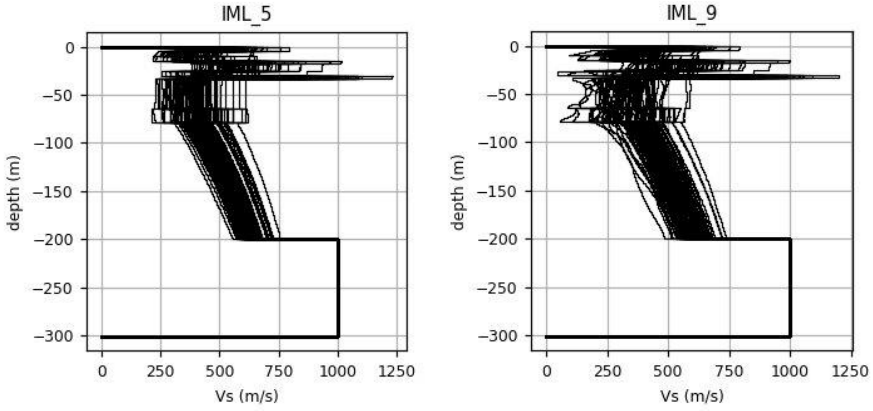

(b)

Figure 1.1 Shear Wave Velocity (Vs) Profile for two IML 5 and 9: (a) Best Estimate (b) Best Estimate with Uncertainties

The ground motions used in the fragility assessment for both scalar and vector intensity measures correspond to intensity measure levels (IMLs) 5, 6, 7, 8, and 9 for the BEU case. This selection results a total of 500 ground motions and ensures that uncertainties are thoroughly addressed.

2 Description of the Developed Simplified Model and Structural Uncertainties

To address the high computational demands associated with determining the optimal combination of intensity measures and propagating uncertainties, a simplified model of the Diesel Generator Building (DGB) was developed.

2.1 Diesel Generator Building (DGB Model)

The Diesel Generator building at the Zaporizhzhia NPP, consists of three identical block-cells, each housing a diesel generator. 1DGB-1 is in a separate block-cell, while 1DGB-2 and 1DGB-3 share a three block-cell structure (Figs 2.1 and 2.2).

The DGB foundation is a 700 mm thick monolithic reinforced concrete slab made of M200 concrete, with a base elevation of -7.900 m. The external and internal load-bearing walls are constructed from three-layer prefabricated monolithic reinforced concrete blocks. The prefabricated concrete is 80 mm thick, with overall wall thicknesses of 900 mm (external) and 600 mm (internal). The reinforcement is A I and A III grade, and the concrete is M200 and M300. The floors are prefabricated monolithic slabs made of M200 and M300 concrete, 600 mm thick, with permanent formwork and bottom reinforcement. The channel covers are made of VSt3kp2 steel. The roof slab is also prefabricated monolithic, with a total thickness of 900 mm, reinforced with spatial reinforcement cages. The building is equipped with overhead cranes and hoists. The roofing consists of a three-layer roll material made of RM-350 roofing felt on bitumen mastic, over foam concrete insulation (80 mm) and a cement-sand screed (15 mm).

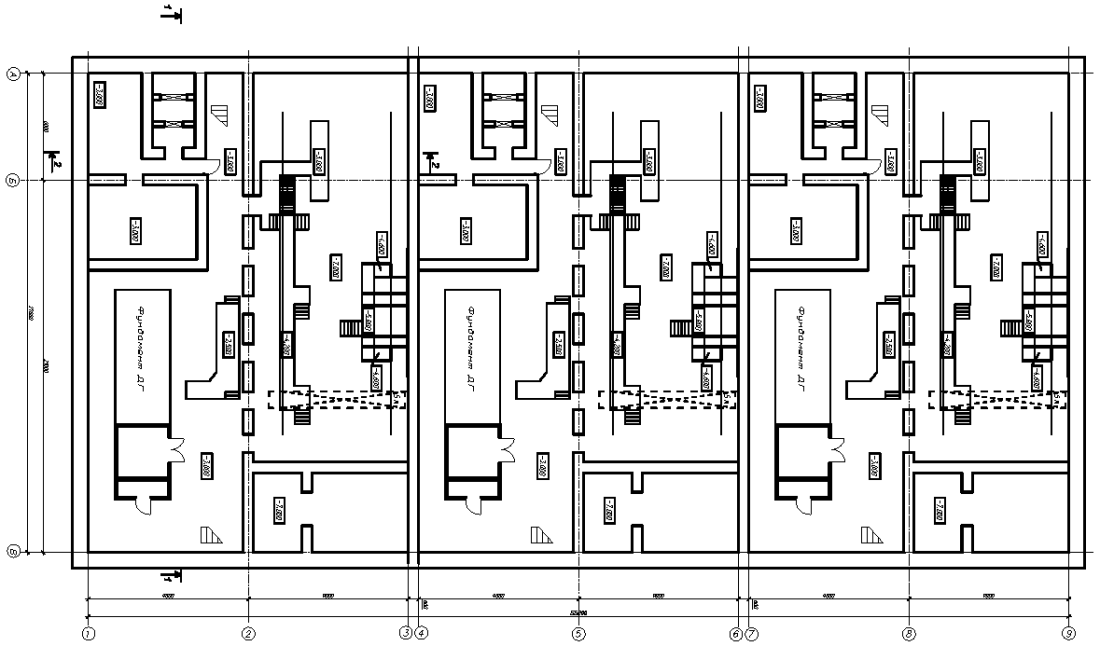

Figure 2.1 Diesel Generator Building (1DGB-2,3) plan, elevation -3,000; -7,000

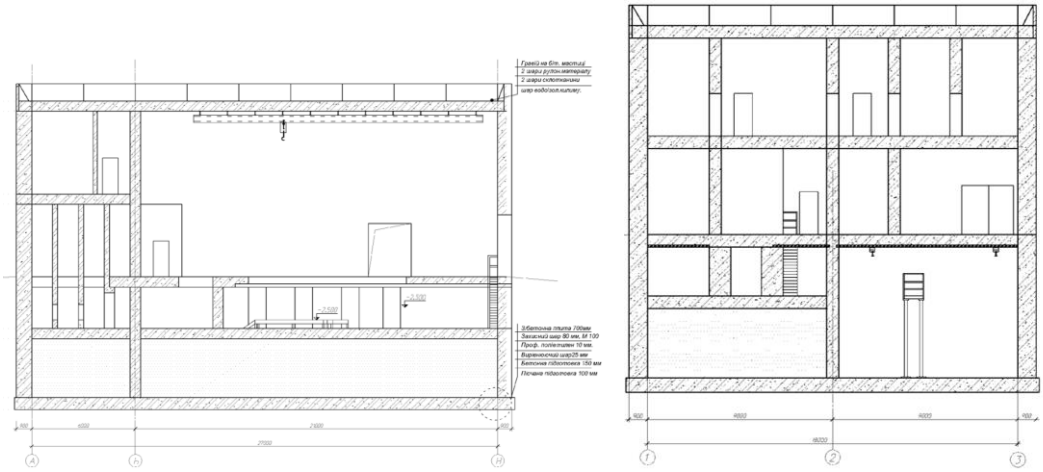

(a) (b)

Figure 2.2 Diesel Generator Building (1DGB): (a) Section Cut 1-1 (b) Section Cut 2-2

To develop a simplified model, it is essential to obtain the pushover curve and the modal results, which characterizes the relationship between base shear and displacement, and the dynamic characteristics of the structure. This curve serves as a key input to define the capacity of the simplified model. To achieve this, a comprehensive numerical model of the Diesel Generator Building (DGB) was developed in STKO software [2,3], incorporating material nonlinearity and appropriate element types. This complex model ensures an accurate representation of the structural behaviour necessary for defining the simplified model's capacity.

The mechanical characteristics of the used materials for the DGB development are presented in table 2.1, Figure 2.3 shows the 3D finite element model of the reactor building and its inside.

Table 2.1 Materials properties of the DG building

Material	Density (kg/m^3)	Young's Modulus (MPa)	Poisson's Ratio	Compressive Strength (MPa)
Concrete 01	2500	25000	0.2	17
Reinforcement	7850	210000	/	500

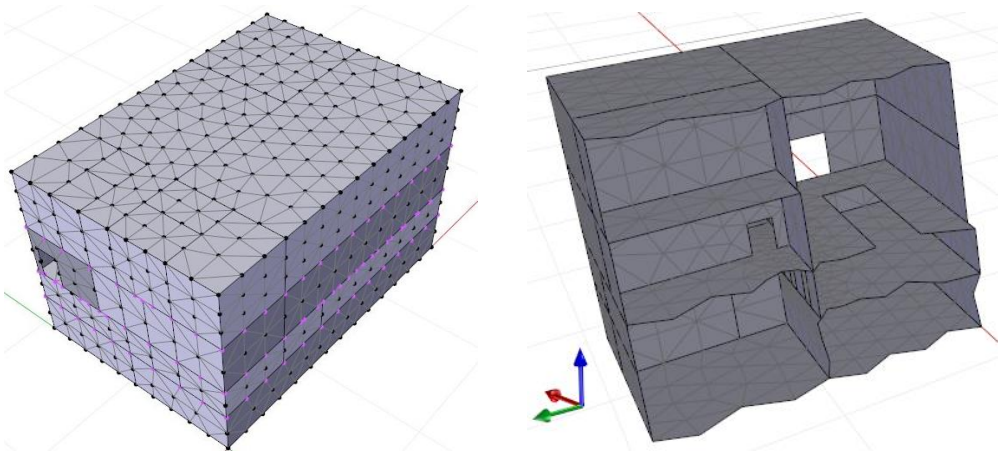

(a) (b)

Figure 2.3 (a) Finite Element (FE) model of the Diesel Generator Building (b) Cross-sectional view of the Diesel Generator Building's FE model

2.2 Diesel Generator Building Simplified Model

The DGB simplified model has four lumped masses assigned at the same structural levels as the DGB complex model. The elastic beam-column element available in the OpenSees library [3] was used to connect the node masses. The nonlinearity in the DGB simplified model was incorporated through a spring element at the base of the multi-degree-of-freedom system, using a hysteretic material in a zero-length element. This setup allows the model to simulate the degradation of structural capacity after cyclic loading.

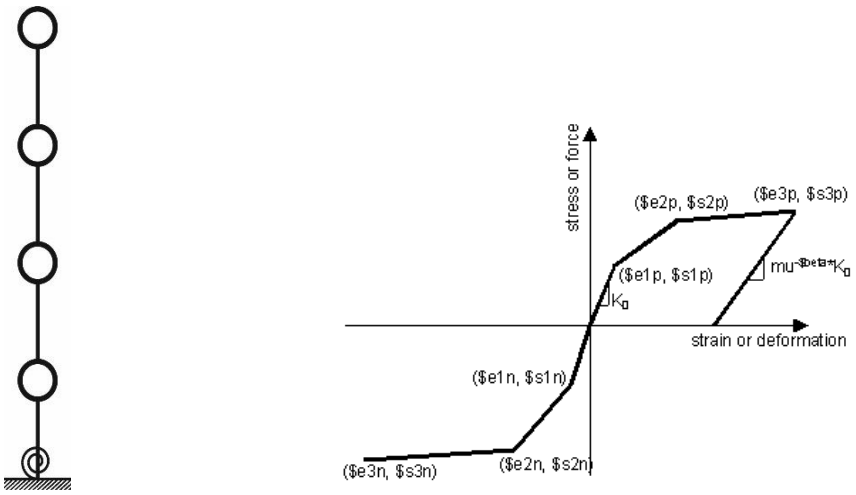

Figure 2.4 (a) DGB simplified Model (b) the material hysteric behavior of the zero-length element [3]

To ensure that the simplified model accurately reflects the dynamic characteristics of the complex DGB model, a modal analysis of the Diesel Generator Building was conducted. An iterative process was carried out to adjust the properties of the simplified model elements—such as cross-sectional areas and elastic modulus—to align with the modal results of the complex model [4–6]. It is also worth noting that only the fundamental modes in each direction were considered, as these were deemed sufficient after observing the mass participation in each mode, which exceeded 70%.

Table 2.2 Comparison between the modal results DGB simplified and complex models

Modes	DGB-MDOF Frequency (Hz)	DGB-Complex Model Frequency (Hz)
Translational mode, along X dir	12.06	12.00
Translational mode, along Y dir	16.27	16.27
Rotational mode, Z dir	32.71	32.72

The nonlinearity in the simplified model was incorporated based on the nonlinear static analysis [7] performed on the DGB complex model, from which the relationship between base shear forces and displacement in both x and y directions was extracted. To validate the simplified model, an additional pushover analysis was conducted on the simplified model. This comparison is shown below.

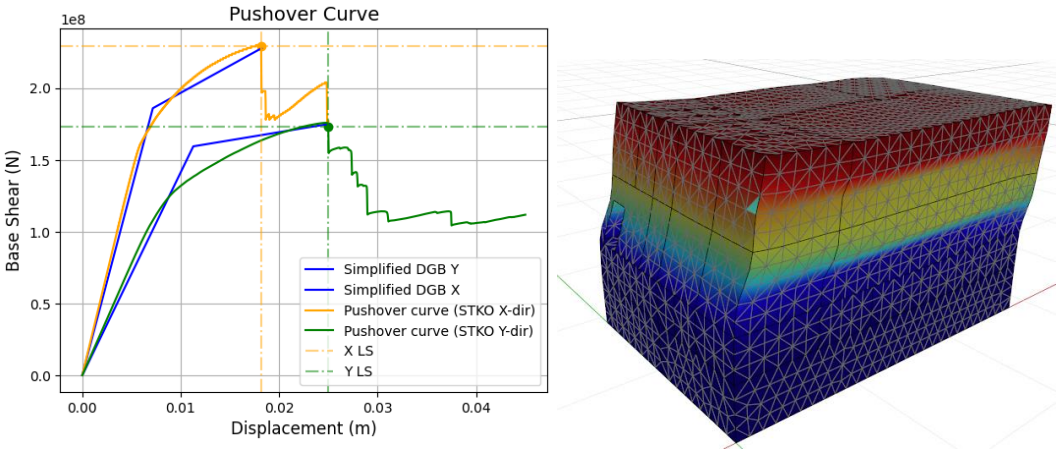

Figure 2.5 (a) Comparison between the simplified and complex models' capacity curves (b) Deformation of the complex DGB model at the final step of the pushover analysis

This comparison, illustrated in Fig 2.5, demonstrates the alignment of the simplified model's response with that of the complex model, confirming its accuracy in capturing essential structural characteristics.

3 Fragility Based on Single-Parameter Intensity Measures

This section outlines the workflow used to determine the optimal intensity measure, beginning with the uncertainties incorporated into the studied simplified model. It covers the selection of intensity measures, the various fragility methodologies employed, and the range of engineering demand parameters (EDPs) and structural behavior stages considered. The goal is to identify an intensity measure that minimizes uncertainty, providing a baseline for comparison with the vector fragility approach presented in the following section.

3.1 Uncertainty Modelling and Sampling Approach

To address the propagation and quantification of uncertainties in the structural response, uncertainties related to structural properties were incorporated, assuming a log-normal distribution. A total of three variables were sampled using a Latin Hypercube Sampling Design [8]. Notably, uncertainties associated with the structure's fundamental period are inherently included when accounting for uncertainties in structural capacity, due to the characteristics of the Hysteretic material used in the model.

Table 3.1 Incorporated Uncertainties within the Simplified Model [9,10]

Variables	Definition	Standard Deviation
Mpy	Moment Capacity in Y directions	0.15
	Damping	0.3

3.2 Selected Intensity Measures for Scalar and Vector Fragility study

Intensity measures are parameters used to represent the ground motions inputs, these intensity measures could be categorized into several categories such as structure and non-structure specific.

In the context of steel moment frames, a study assessing seismic fragility identified effective intensity measures (IMs) for frames ranging from 2 to 20 stories in height. By evaluating 20 IMs with maximum interstory and roof drifts as demand parameters, the study concluded that Housner intensity (HI), peak ground velocity (PGV), and spectral pseudo-acceleration at the fundamental period (PSa(T1)) were particularly effective. Specifically, HI was optimal for interstory drift in frames between 2 and 12 stories, PGV was preferable for 12-20 story frames, and PSa(T1) was most suitable for roof drift across all frames. Conversely, peak ground acceleration (PGA) was found unsuitable for these steel structures [11].

Research on seismic demand models for circular tunnels in soft soil employed time history analyses to evaluate 18 IMs, indicating that peak ground acceleration (PGA) was optimal for shallow tunnels, while peak ground velocity (PGV) was better suited for deeper tunnels [12].

A study on base-isolated nuclear power plant (NPP) structures revealed that the effectiveness of IMs varies according to the engineering demand parameters (EDPs) considered. For maximum floor displacement (MFD) and maximum isolator displacement (MID), velocity spectrum intensity, Housner intensity, peak ground velocity, and spectral velocity were identified as the most effective IMs. Meanwhile, peak ground acceleration and acceleration spectrum intensity proved optimal for maximum floor acceleration (MFA). Cumulative absolute velocity, however, was deemed unsuitable for predicting exceedance of the operating basis earthquake level [13].

Another analysis focusing on the APR1400 nuclear plant's reactor containment building (RCB) evaluated seismic performance using 90 ground motions and 20 IMs. Spectral acceleration, spectral velocity, and effective peak acceleration emerged as the most efficient IMs, whereas peak ground displacement and velocity spectrum intensity exhibited weaker correlations with performance outcomes [14].

Another investigation into the seismic response of a Canada Deuterium Uranium (CANDU) containment structure found that spectral acceleration (Sa) and spectral displacement (Sd) at the fundamental period (T1) were the most effective IMs for assessing seismic damage [15,16].

In summary, based on these studies and the findings from deliverable 6.3, the commonly used intensity measure, peak ground acceleration (PGA), is suitable for structures with a high dominant frequency, providing a good correlation with their response. However, in other cases, PGA was found to be less effective. For structures with intermediate fundamental frequencies, peak ground velocity (PGV) is a more suitable measure. Conversely, peak ground displacement (PGD) is better aligned with structures dominated by low-frequency structural fundamental mode.

However, the conclusions about the optimal intensity measures (IMs) from these studies were primarily based on observing the dispersion, or the coefficient of variation (COV), of the fragility curves generated from the case studies. To gain a more comprehensive understanding, it may be beneficial to include additional statistical parameters to evaluate the goodness of fit. For this sake, a total of 19 intensity measures presented in Table 3.2 were selected, for the investigation of the optimal scalar IM while the optimal vector IM was assessed based on the performance of different IM combinations. This analysis was conducted using the simplified model of the Diesel Generator Building as a case study.

Table 3.2 Selected Intensity Measure for the case study

IM	Definition	Reference
$\mathbf{PGA} = \mathbf{max}\,(\lvert\mathbf{a}(\mathbf{t})\rvert)$	Peak ground acceleration	
Sa(T_1)	Spectral Acceleration at the fundamental structural period	[18]
SaAvg (0.1-0.2s)	Average Spectral Acceleration between the periods of 0.1 and 0.2 s	[19]
SaAvg (0.1-0.4s)	Average Spectral Acceleration between the periods of 0.1 and 0.4 s	
SaAvg (0.05-0.4s)	Average Spectral Acceleration between the periods of 0.05 and 0.4 s	
$\mathbf{PGV} = \mathbf{max}\,(\lvert\mathbf{v}(\mathbf{t})\rvert)$	Peak ground velocity	[20]
$\mathbf{CAV} = \int_0^{\mathbf{t_{max}}} [\mathbf{a}(\mathbf{t})]\mathbf{dt}$	Cumulative absolute velocity	[21]
SCAV = $\int_0^{tf} \lvert\mathbf{a}(\mathbf{t})\rvert\, \boldsymbol{dt} + \int_{i-1}^{ti} \lvert\mathbf{a}(\mathbf{t})\rvert\, \boldsymbol{dt}$	Standardized cumulative absolute velocity	[20]
SI = $\int_{0.1}^{2.5} S_v(\xi, \mathbf{T})\boldsymbol{dT}$	Spectral intensity (m.s-1)	[22,23]
$\mathbf{HI} = \int_{0.1}^{2.5} \mathbf{PSV}(\xi = \mathbf{0.05}, \mathbf{T})\mathbf{dT}$	Housner Intensity	[24]
$\mathbf{I_A} = \frac{\pi}{2\mathbf{g}} \int_0^{\mathbf{T_d}} \mathbf{a}(\mathbf{t})^2\mathbf{dt}$	Arias Intensity	[25]
(5-95% of the Arias intensity)	Husid duration (s)	[26]
(5-75% of the Arias intensity)	Trifunac duration (s)	[26]
$E_{Ia} = E_{kr} + E_d + E_s = \int_0^{t_f} \boldsymbol{m} \cdot \ddot{\boldsymbol{u}}_t(t) \cdot \dot{\boldsymbol{u}}_g(t) \cdot \boldsymbol{dt}$	Relative input energy	[27]
$S_v(T_1) = \mathbf{max}\,(\lvert\dot{u}_g(\mathbf{t}, \xi, T_1)\rvert)$	Spectral Velocity	[22,23]
$\mathbf{CAD} = \int_0^{\mathbf{t_{max}}} [\mathbf{v}(\mathbf{t})]\mathbf{dt}$	Cumulative absolute Displacement	[28]
$\mathbf{N_p} = \frac{\mathbf{Sa_{avg}}(\mathbf{T_1} \ldots \mathbf{T_N})}{\mathbf{Sa}(\mathbf{T_1})}$		[29]
$\mathbf{EPA} = \frac{\mathbf{1}}{\mathbf{2,5}} \frac{\mathbf{1}}{\mathbf{0,4}} \int_{0,1}^{0,5} \mathbf{Sa}(\xi = \mathbf{5\%}, \mathbf{T})\mathbf{dT}$	Effective Peak Acceleration	[30]
$\mathbf{PGD} = \mathbf{max}\,(\lvert\mathbf{d}(\mathbf{t})\rvert)$	Peak ground displacement	

3.3 Fragility Methodologies

Determining the failure probability in relation to a preferred intensity measure—represented by the fragility curve—is a critical step in the Seismic Probabilistic Risk Assessment (SPRA) process [31]. Various methods from existing literature can be utilized to achieve this, including Cloud Analysis, Incremental Dynamic Analysis, Multiple Stripe Analysis [19,32–34].

Within this report, two primary approaches are applied: Cloud Analysis and Incremental Dynamic Analysis. These approaches differ in how they handle the selected ground motions. In the Cloud Analysis approach, ground motions are used in their original, unscaled form, which maintains consistency with previous ground motion simulation studies. In contrast, the Incremental Dynamic Analysis approach involves scaling ground motions until the desired deformation level is reached. This evaluation was further expanded to include various types of engineering demand parameters, specifically drift and acceleration.

To determine the parameters of the fragility curves, specifically the median and dispersion, the dataset obtained from the nonlinear time history analysis (NLTHA)—which captures the relationship between the response and input for both the Cloud and Incremental Dynamic Analysis (IDA) approaches—is analyzed using two methods: regression and maximum likelihood estimation.

3.3.1 Regression on IM and EDP

The regression method [35] requires a sample of N input-output pairs, (α_i, y_i) , i=1,….,N , where the input is the ground motion indicator or seismic intensity level α_i and the output is the continuous damage y_i, The continuous engineering demand parameter Y is modelled as lognormal random variable :

$$Y = b\,\alpha^c \eta \qquad (Eq.1)$$

where η is a lognormal random variable with a median of 1 and a logarithmic standard deviation σ. It is assumed that the structure fails or reaches a certain damage level when the variable Y exceeds a threshold D_S such that $P_f(\alpha)=P(Y>D_S|\alpha)$. The parameters b, c, and σ can be conveniently determined by linear regression in log-space:

$$\ln Y = \ln b + c \ln \alpha + \sigma\varepsilon \qquad (Eq.2)$$

where $\sigma\varepsilon = \ln\eta$, is a centred normal random variable with standard deviation σ, the latter is obtained as the standard deviation (std) of the regression error. Moreover, defining $D_s=bA_m^c$, we have:

$$A_m = \exp\left(\frac{\ln\left(\frac{Ds}{b}\right)}{c}\right) \qquad (Eq.3)$$

In consequence, the fragility curve is described by a lognormal distribution with a median equal to the seismic capacity Am and the lognormal standard deviation $b=\sigma/c$ such that:

$$pf(\alpha) = \Phi\left(\frac{c\,\ln\left(\frac{\alpha}{Am}\right)}{\sigma}\right) = \Phi\left(\frac{\ln\left(\frac{\alpha}{Am}\right)}{\sigma/c}\right) \qquad (Eq.4)$$

One key advantage of the linear regression approach is its ability to be utilized even when no failures are observed. It doesn't inherently require the scaling of accelerograms and remains effective, even with smaller sample sizes. Although linear regression can be applied to any dataset, it does involve extrapolating the behaviour in cases where no failures are detected.

Despite the simplicity of this approach, which makes it suitable for practical applications, it is important to note that it assumes a constant standard deviation across the entire intensity measure (IM) range. This assumption leads to the estimation of dispersion being uniform across different stages of structural

performance (both linear and nonlinear). Therefore, maximum likelihood estimation (MLE) is also employed in this investigation to address this limitation.

3.3.2 Maximum Likelihood Approach

Shinozuka et al. (2000) [36] introduced a statistical approach to estimate the median and dispersion of fragility curves using a set of binary data Y : where all the points exceeds a defined threshold take a value y_i=1 ,otherwise 0. Then the variable Y is assumed to follow a binomial or a Bernoulli distribution. Based on this definition, the likelihood of the fragility function follows the following form:

$$L(\alpha,\beta) = \prod_{i=1}^{N} [P_f(im_i,\alpha,\beta)]^{y_i} [1 - P_f(im_i,\alpha,\beta)]^{1-y_i} \qquad (Eq.5)$$

This function L is then maximized using an algorithm, leading to an estimate of the fragility parameters α and β.

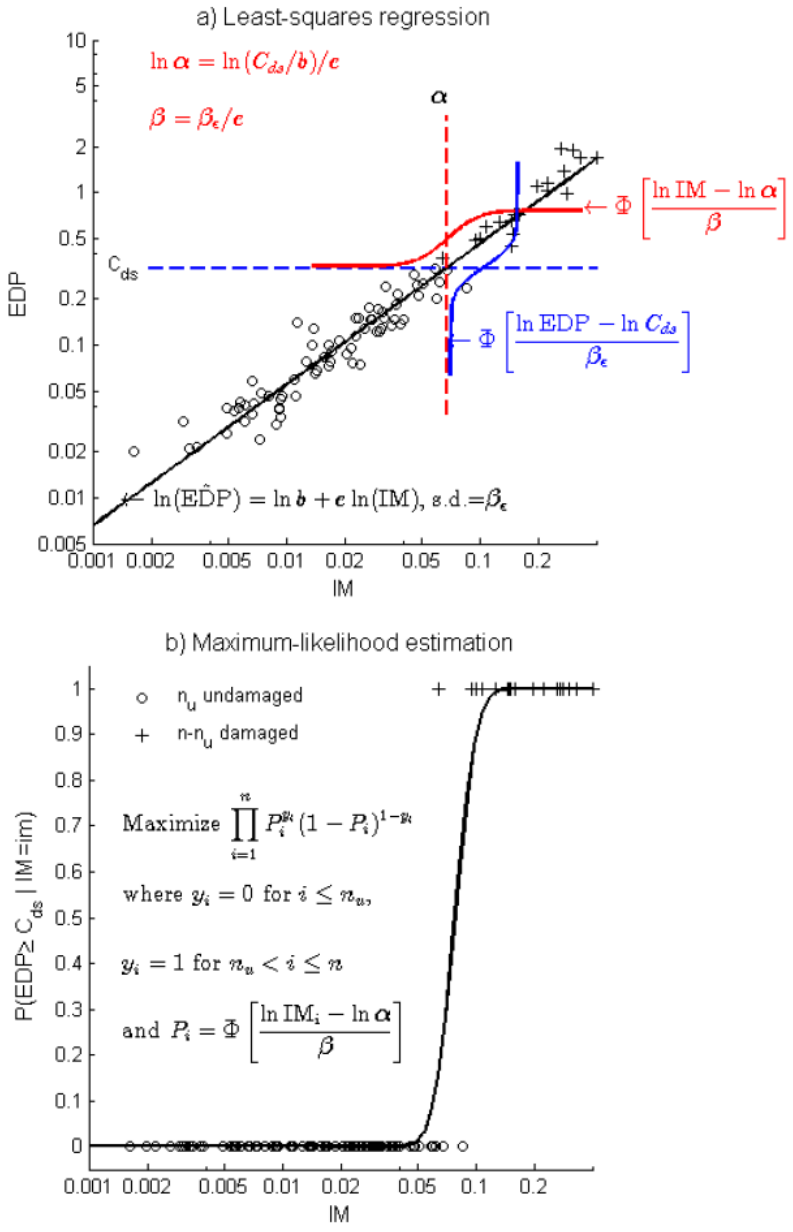

Figure 3.1 Estimation of the fragility parameter (a) Regression (b) Maximum Likelihood Estimation

3.4 Seismic Fragility Analysis for Low-Damage States Based on Scalar IM

In this section, the results of the time history analysis for the diesel generator building case study are presented. The interpretation of these results is organized into four parts: the cloud approach using both Regression and MLH, and IDA using Regression and MLH.

other statistical parameters are introduced here:

(a) Akaike Information Criterion (AIC):

This criterion measures how well a model fits the data by assigning a numerical score. The Akaike Information Criterion (AIC) [37] adjusts for the number of parameters used in the model, represented by k, to avoid over-complicating the model. For scalar-IM fragility curves, k is 2 (i.e., parameters a and β). The AIC formula is as follows:

$$AIC = 2k - 2\ ln\ L \qquad (Eq.6)$$

where L is the likelihood function of the fragility model.

(b) Area Under the ROC curve (AUC):

The Area Under the Curve (AUC) [38] measures how well a model distinguishes between classes. It ranges from 0 to 1, with higher values indicating better performance, where 1 means perfect accuracy and 0.5 is no better than random guessing. Note that, The Receiver Operating Characteristic (ROC) curve is a graphical representation of a classification model's performance, showing the trade-off between true positive rate (sensitivity) and false positive rate, helping to assess its ability to distinguish between classes at different threshold levels.

3.4.1 Regression Analysis for Cloud Method

After conducting the dynamic analysis on the case studies, including uncertainties and a set of 500 ground motions, multiple simulations were performed for each ground motion to account for uncertainty propagation. Two engineering demand parameters—Drift and Acceleration— [39,40] were used to evaluate their correlation with the selected Intensity Measure (IM).

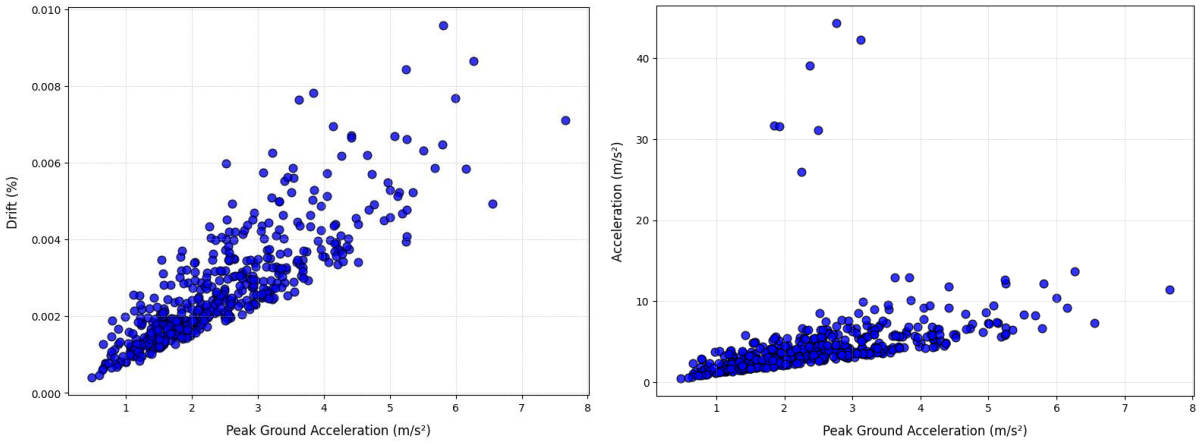

(a) (b)

Figure 3.2 Relationship between the EDP and IM: (a) PGA versus Drift (b) PGA versus Acceleration

From the previous plot, Drift increases almost in a linear relationship with PGA, showing a strong and

predictable relationship. In contrast, Acceleration appears more scattered, indicating a weaker correlation. This suggests Drift is a more reliable indicator of PGA's impact.

To assess the correlation of spectral acceleration not only at the structural period but across various fundamental periods Sa(T), the responses were analysed in relation to different spectral accelerations. This involved calculating dispersion based on fragility analysis (assuming the roof drift threshold of 4‰), as well as evaluating additional parameters such as AIC and AUC.

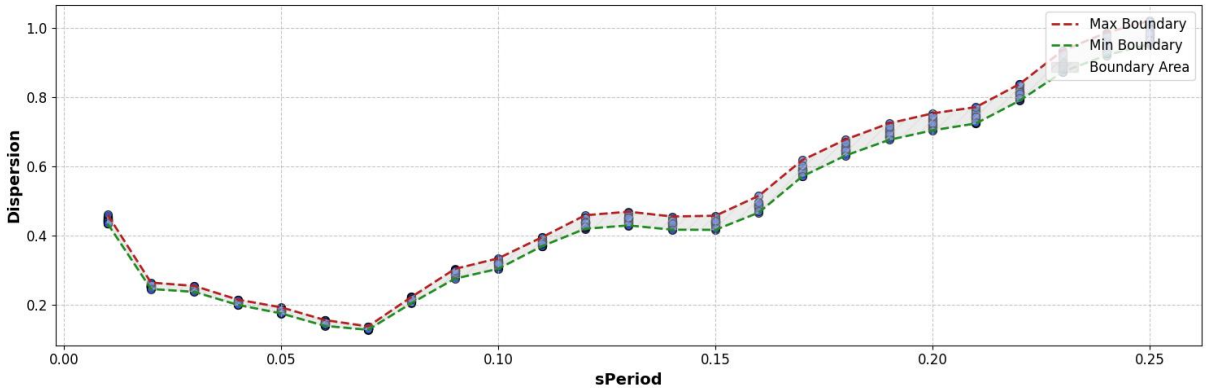

(a)

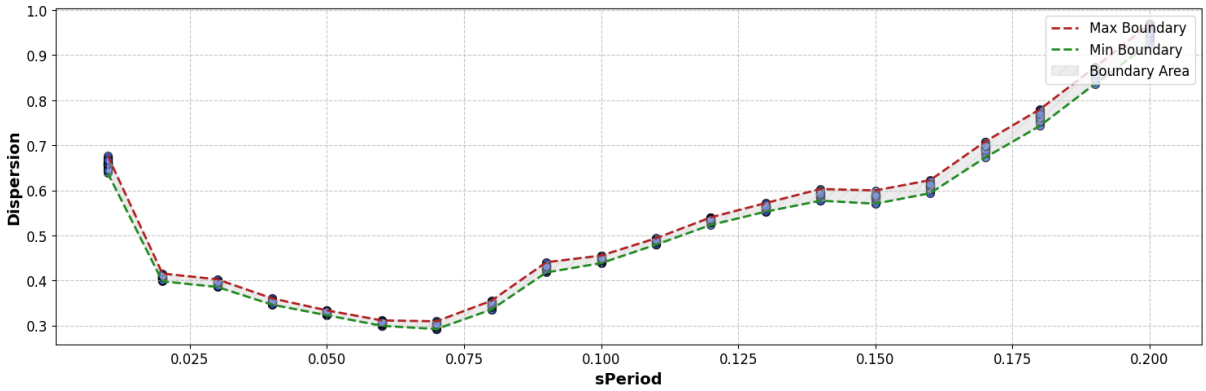

(b)

Figure 3.3 Variation of Dispersion with Respect to Spectral Acceleration at Different Periods: (a) Using Drift as EDP, (b) Using Acceleration as EDP

Note: The Max Boundary represents the upper limit of observed uncertainties, while the Min Boundary represents the lower limit.

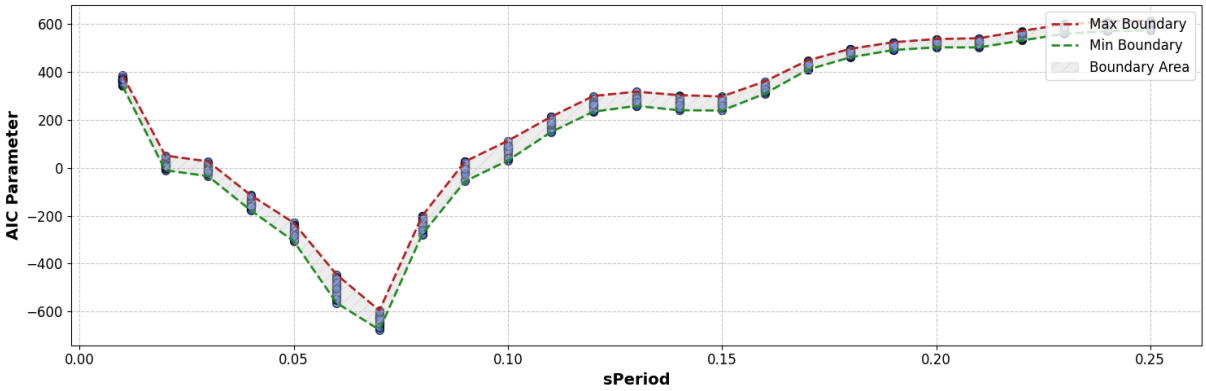

(a)

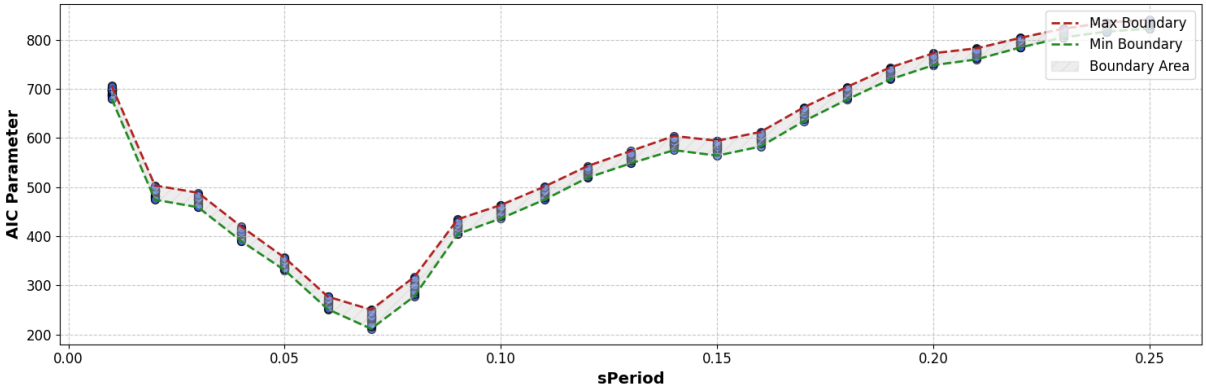

(b)

Figure 3.4 Variation of AIC parameter with Respect to Spectral Acceleration at Different Periods: (a) Using Drift as EDP, (b) Using Acceleration as EDP

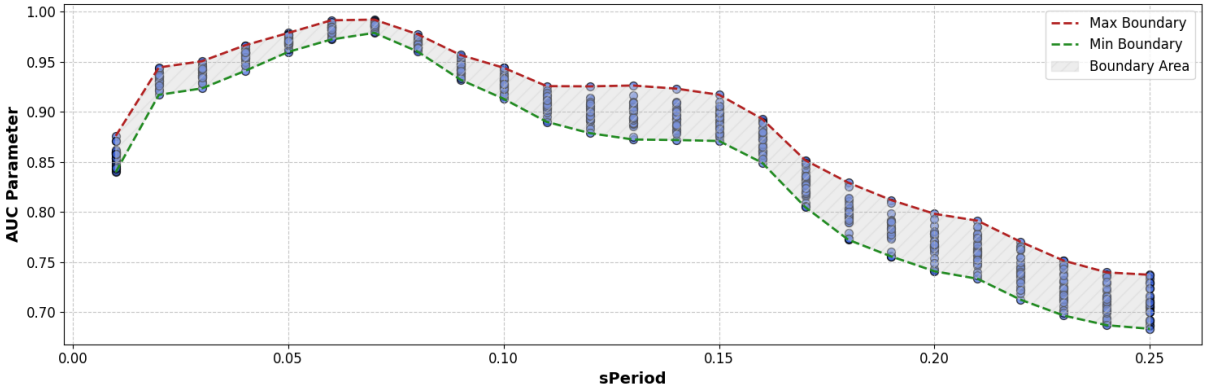

(a)

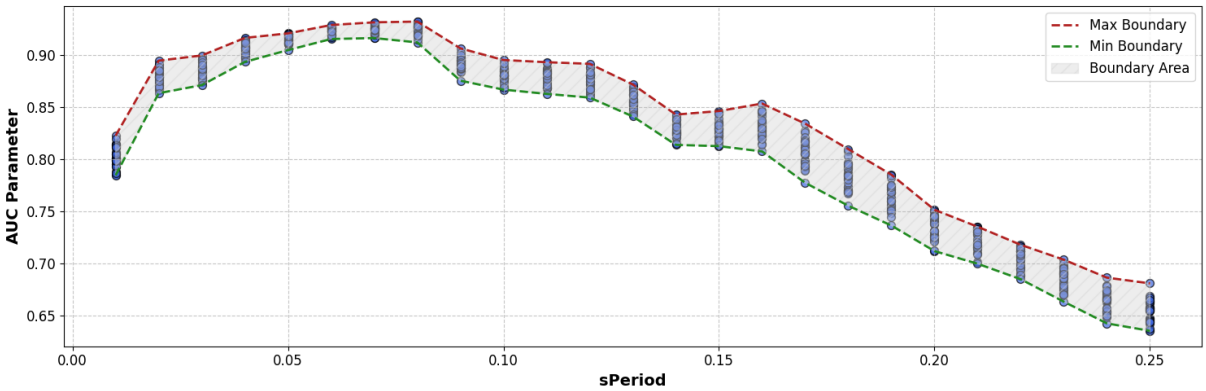

(b)

Figure 3.5 Variation of AUC parameter with Respect to Spectral Acceleration at Different Periods: (a) Using Drift as EDP, (b) Using Acceleration as EDP

From the dispersion plot, it can be observed that the dispersion values obtained when using acceleration as the EDP are generally higher across all cases of spectral acceleration periods compared to using drift. Notably, the dispersion is lower when the spectral acceleration period is close to the translational fundamental period of the structure (Y Dir). Specifically, at the fundamental period Sa(T_1) both drift and acceleration display their lowest dispersion with values of 0.17, 0.3 respectively.

Similar to the dispersion plots, the variation in AIC values with spectral acceleration across different fundamental periods is generally higher when using acceleration as the EDP compared to drift. For the AIC parameter, a lower value indicates a better-fitting model, and in this analysis, the lowest AIC values occur at the fundamental period for both EDPs, indicating the best model fit around this period. Similarly, for the AUC parameter, values closer to 1 suggest a better fit, which is also observed at the structure's fundamental period. These results indicate that spectral acceleration at the fundamental period provides the most reliable model fit compared to other periods.

The ROC curves highlight the effectiveness of SaAvg (0.05–0.15s) versus PGV and PGD as Intensity Measures, demonstrating both sensitivity and specificity. SaAvg (0.05–0.15s) (blue) shows a steep rise and high AUC, indicating strong predictive accuracy and high specificity. In contrast, PGV ,PGD has a slower rise and lower AUC, showing weaker performance.

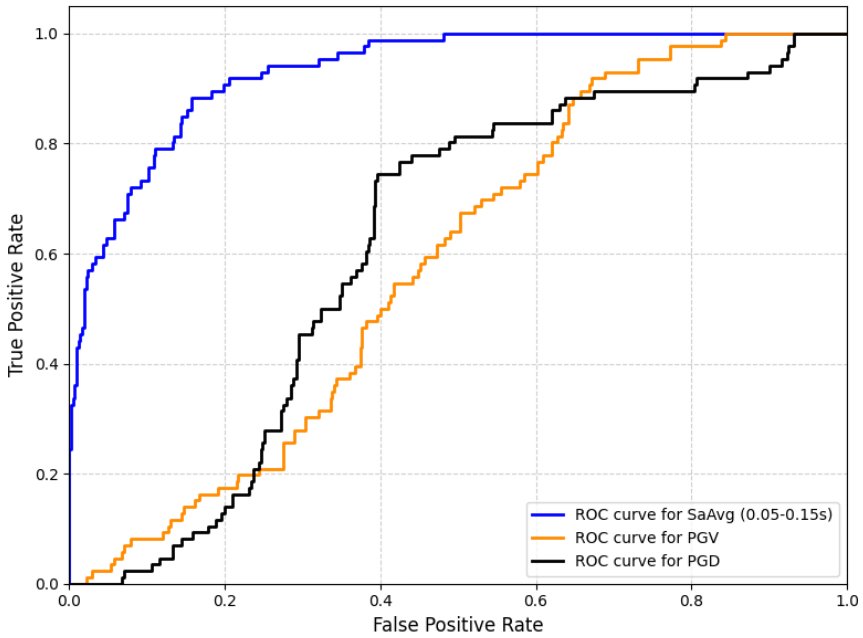

Figure 3.6 ROC Curves Comparing Predictive Performance of SaAvg (0.05–0.15s) and PGV

The performance of the other intensity measures discussed in Section 3.2 is evaluated using these parameters across various EDPs. A summary of the results is provided on the table below.

Table 3.3 Summary of Intensity Measure Performance for Drift and Acceleration as EDPs (Cloud-Regression)

	Case 1: Drift as an EDP			**Case 2: Acceleration as an EDP**		
IM	Beta	AIC	AUC	Beta	AIC	AUC
PGA	0.47	409.08	0.82	0.67	697.91	0.79
Sa(T1)	0.17	-362.11	0.95	0.3	233.68	0.92
SaAvg (0.1-0.2s)	0.38	231.97	0.89	0.5	532.27	0.85
SaAvg (0.1-0.4s)	0.56	464.68	0.79	0.77	727.99	0.75
SaAvg (0.05-0.15s)	0.27	-10.69	0.93	0.38	381.43	0.9
PGV	2.3	747.95	0.58	4.67	908.55	0.57

CAV	/	773.16	0.52	/	915.42	0.51
SCAV	4.07	760.5	0.54	/	909.34	0.53
SI	4.52	771.83	0.51	/	916.76	0.49
HI	/	781.1	0.59	/	906.38	0.61
AI	1.92	651.15	0.3	2.64	843.24	0.32
HD	/	/	/	/	/	/
TD	/	/	/	/	/	/
RE	1.34	467.88	0.15	1.38	614.79	0.13
CAD	/	769.77	0.62	/	889.99	0.63
SV	/	768.38	0.56	/	889.99	0.63
Np	2.68	780.12	0.44	2.4	913.98	0.44
EPA	0.68	544.59	0.25	0.95	783.27	0.29
PGD	/	767.06	0.62	/	/	/

Note: A slash (/) in the table indicates that the corresponding Intensity Measure (IM) did not provide a good fit for the selected Engineering Demand Parameter (EDP).

Based on the table, the optimal Intensity Measure (IM) for both cases—using Drift and Acceleration as Engineering Demand Parameters (EDPs)—appears to be $Sa(T_1)$. In Case 1 (Drift as the EDP), Sa(T1) demonstrates the lowest Beta value (0.17), the lowest AIC (-362.11), and the highest AUC (0.95), indicating a strong model fit with minimal dispersion and high accuracy. Similarly, in Case 2 (Acceleration as the EDP), $Sa(T_1)$ again shows the lowest Beta (0.3), a favourable AIC (233.68), and a high AUC (0.92), suggesting it is also optimal when Acceleration is used as the EDP. Although SaAvg (0.05–0.15s) performs relatively well in both cases, with low Beta values and high AUCs, it does not surpass $Sa(T_1)$ in overall model performance. Thus, spectral acceleration at the fundamental period ($Sa(T_1)$) consistently provides the best fit and reliability across different EDPs, making it the preferred IM for this analysis.

3.4.2 Maximum Likelihood Estimation for Cloud Method

For comparison purposes, MLH estimation is applied to the dataset derived from the cloud analysis results. Thresholds are defined for both Engineering Demand Parameters (Drift and Acceleration), categorizing outcomes into collapse and non-collapse. A value of 0 indicates that the structure remained below the defined threshold (non-collapse), while a value of 1 signifies that the threshold was exceeded (collapse).

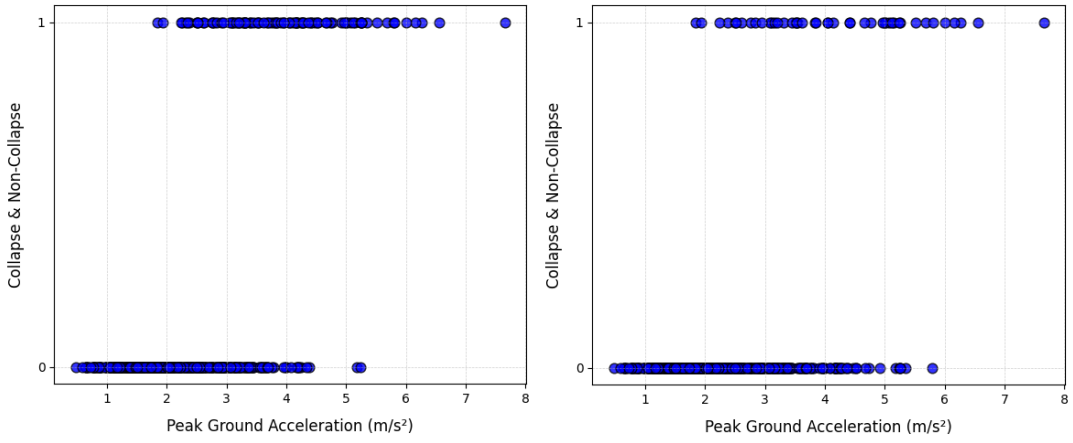

(a) (b)

Figure 3.7 Collapse Assessment with Respect to PGA: (a) Using Drift as the EDP, (b) Using Acceleration as the EDP

The previous plot serves as a basis input for the likelihood function used to determine the optimized fragility parameters, specifically the median and dispersion. Following this, the variation in dispersion across different spectral acceleration periods for both EDPs is illustrated in the Fig 3.8.

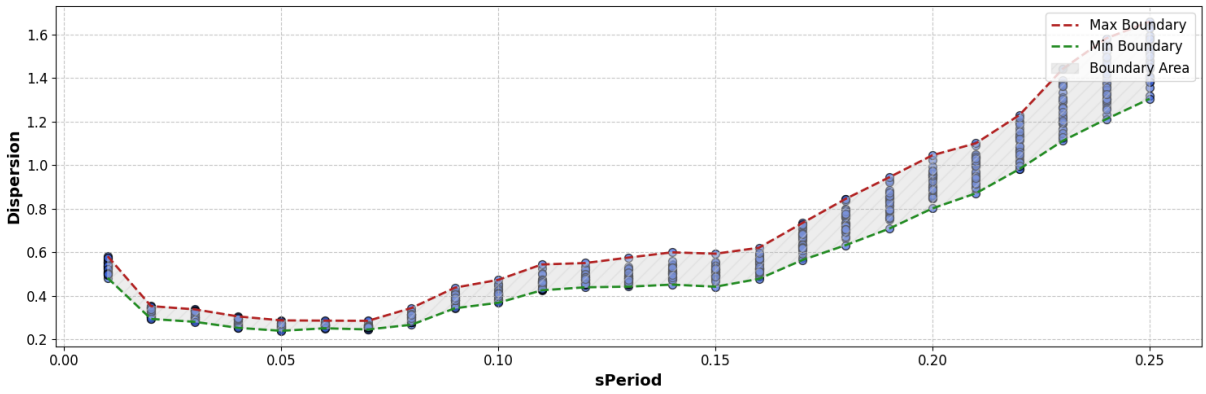

(a)

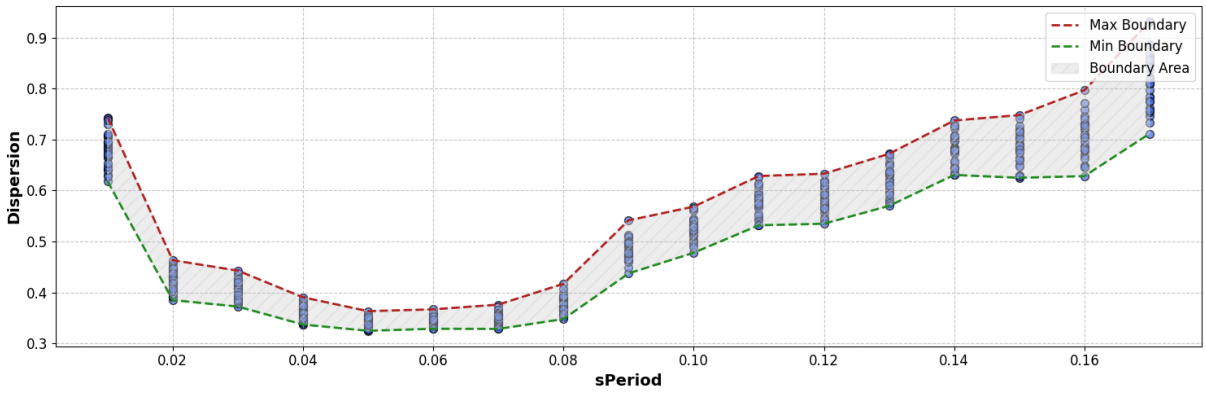

(b)

Figure 3.8 Variation of Dispersion with Respect to Spectral Acceleration at Different Periods: (a) Using Drift as EDP, (b) Using Acceleration as EDP (Cloud-MLH)

Similar to the case of Cloud-regression, the figure 3.8 indicate that the lower dispersion is observed when an IM of a spectral acceleration around the fundamental with optimal to be the spectral acceleration at the fundamental period Sa(T_1) with dispersion values of 0.27 and 0.36 for drift and acceleration as Engineering Demand Parameters, respectively. However, it is important to note that the dispersion observed from the MLH estimation is generally higher compared to the regression case.

Table 3.4 Summary of Intensity Measure Performance for Drift and Acceleration as EDPs (Cloud-MLH)

	Case 1: Drift as an EDP	**Case 2: Acceleration as an EDP**
IM	Dispersion	Dispersion
PGA	0.58	0.73
Sa(T1)	0.27	0.36
SaAvg (0.1-0.2s)	0.42	0.55
SaAvg (0.1-0.4s)	0.72	0.94
SaAvg (0.05-0.15s)	0.31	0.43
PGV	3.28	4.56
CAV	/	/

SCAV	/	/
SI	/	/
HI	/	/
AI	2.36	2.91
HD	/	/
TD	/	/
RE	1.20	1.18
CAD	/	/
SV	/	/
Np	1.34	1.63
EPA	0.92	1.20
PGD	/	/

The results in Table 3.4, which provide information on the correlation of alternative intensity measures using the Cloud MLH approach, align closely with previous findings (Table 3.3). As observed earlier, the dispersion in the EDP–acceleration case is higher than in the EDP–drift case, with the optimal IM for both being the spectral acceleration at the fundamental period Sa(T_1). However, it is also noteworthy that the dispersions resulting from the Cloud MLH approach are generally higher compared to those from the Cloud LR approach.

Finally, as an example, fragility curves for the two intensity measures (PGA and Sa(T1)) using both approaches—Cloud-LR and Cloud-MLH—are presented in Figure 3.9.

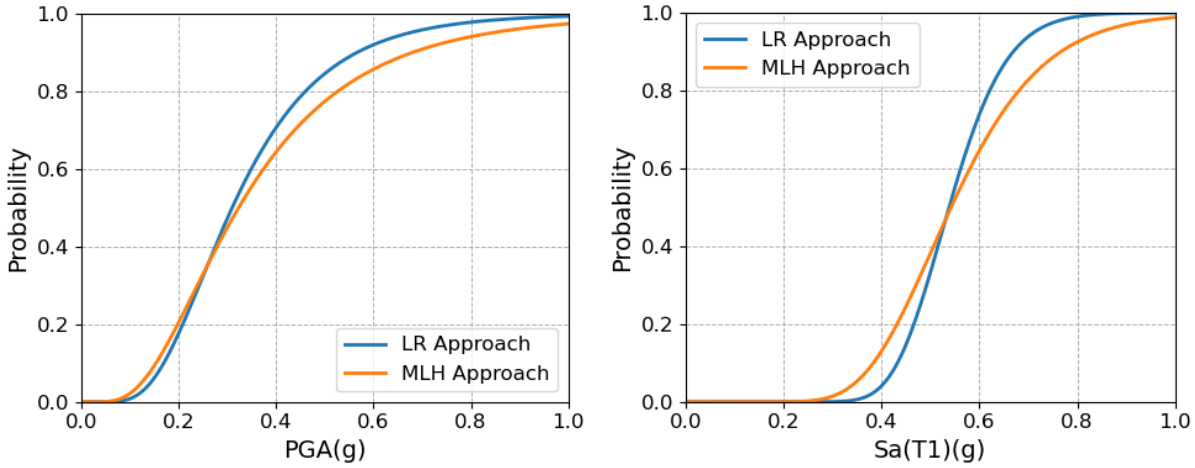

Figure 3.9 Fragility Comparison Based on Cloud LR and MLH Approaches: (a) PGA as Intensity Measure (IM), (b) Sa(T1) as Intensity Measure (IM)

3.4.3 Regression Analysis for Incremental Dynamic Analysis (IDA)

In contrast to the Cloud approach, where ground motions are used without scaling, Incremental Dynamic Analysis (IDA) involves scaling the ground motions incrementally until the desired level of deformation is reached. This method allows for a comprehensive assessment of structural performance across different levels of IM intensity.

A total of 30 ground motions, which is practically used, were selected and incrementally scaled until the

defined threshold was reached. The following figure illustrates the structural responses for both cases of Engineering Demand Parameters (EDP)—Drift and Acceleration—capturing the behaviour of the structure as the intensity measure (IM) increases.

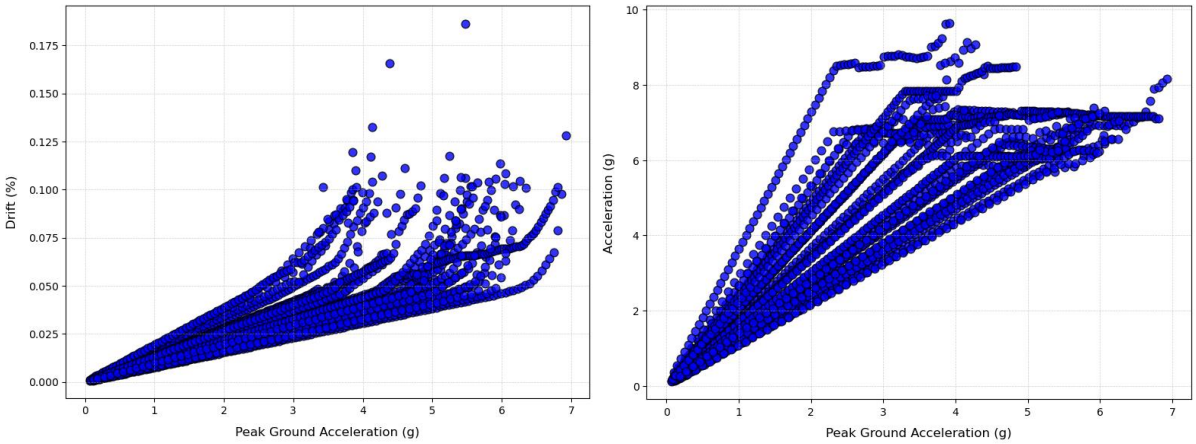

(a) (b)

Figure 3.10 Relationship between the EDP and IM: (a) PGA versus Drift (b) PGA versus Acceleration (IDA Case)

The figure 3.10 illustrate that drift generally increases with PGA, displaying significant variability, especially at higher intensity levels (above 4 g). This variability suggests that drift is more sensitive to ground motion differences, capturing potential non-linear behaviours and structural deformations under higher seismic intensity. On the other hand, the acceleration response shows a more linear and predictable response, with acceleration increasing steadily with PGA but also exhibiting some divergence at very high PGA values.

To evaluate the correlation of spectral acceleration across various fundamental periods Sa(T), the structural responses obtained from IDA analysis were analysed in relation to multiple spectral acceleration values. This analysis included calculating dispersion through fragility analysis and assessing additional parameters such as AIC and AUC to provide a comprehensive understanding of the relationship between response and spectral acceleration.

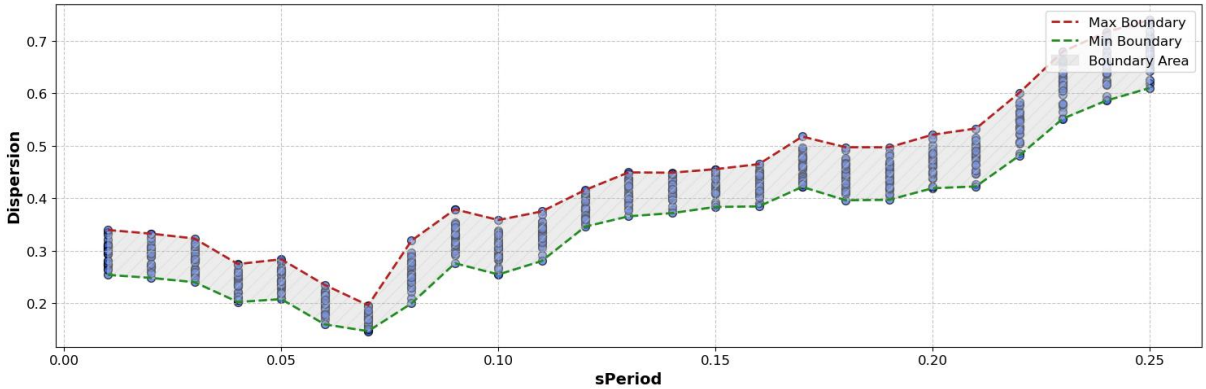

(a)

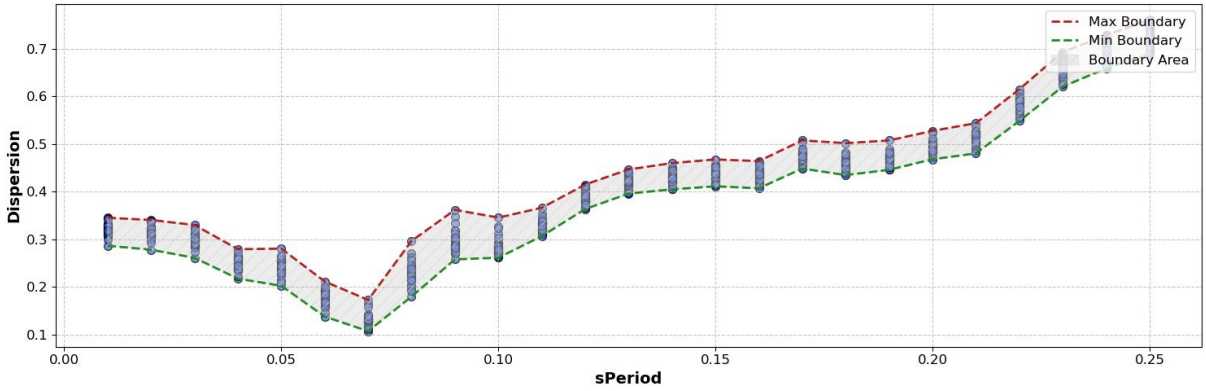

(b)

Figure 3.11 Variation of Dispersion with Respect to Spectral Acceleration at Different Periods: (a) Using Drift as EDP, (b) Using Acceleration as EDP (IDA-LR)

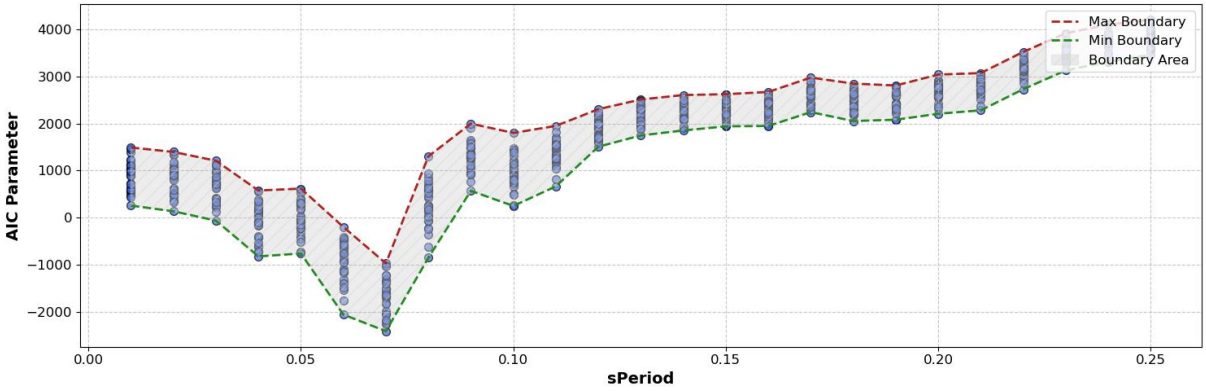

(a)

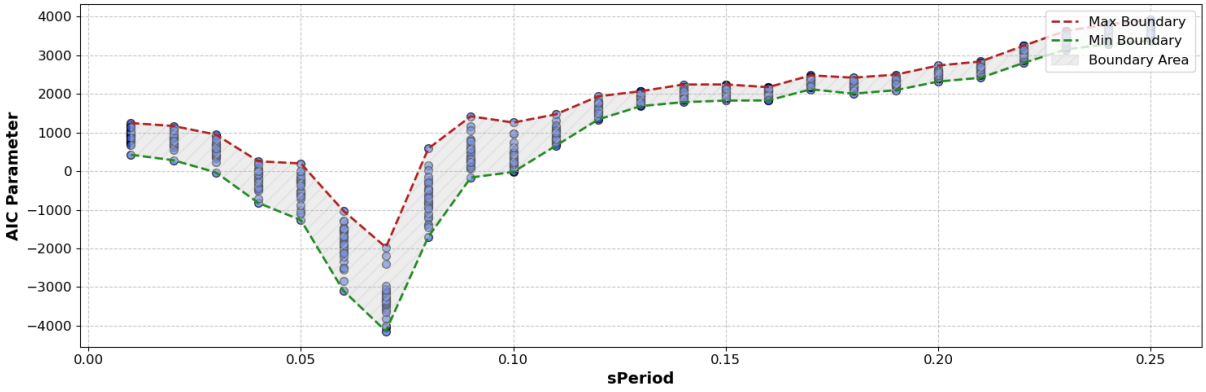

(b)

Figure 3.12 Variation of AIC parameter with Respect to Spectral Acceleration at Different Periods: (a) Using Drift as EDP, (b) Using Acceleration as EDP (IDA-LR)

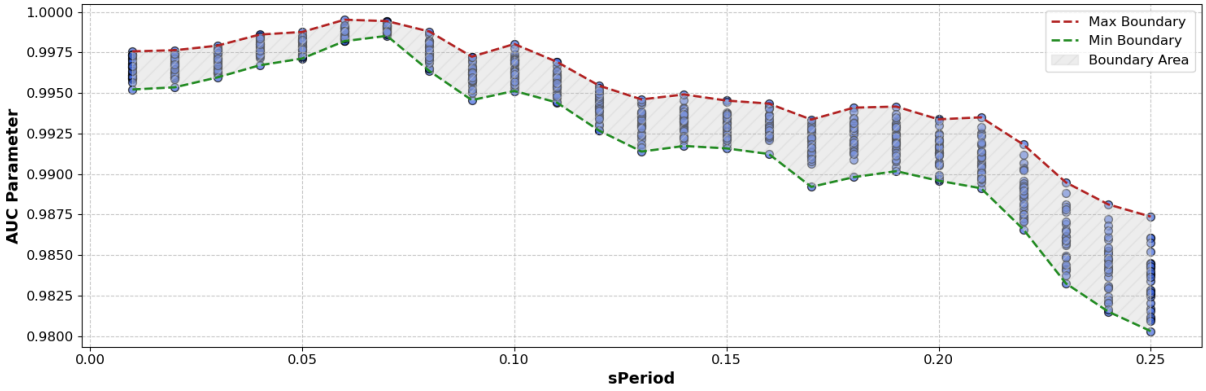

(a)

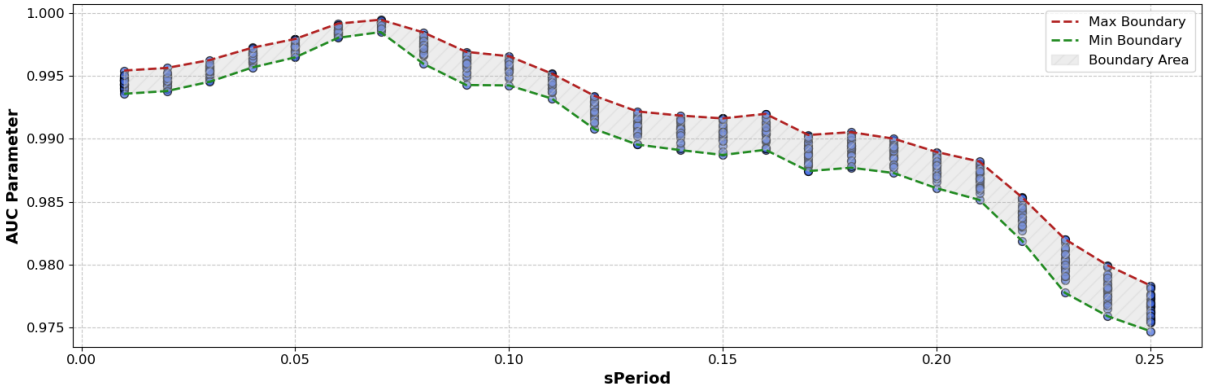

(b)

Figure 3.13 Variation of AUC parameter with Respect to Spectral Acceleration at Different Periods: (a) Using Drift as EDP, (b) Using Acceleration as EDP (IDA-LR)

Comparing the plots from the IDA approach with the cloud analysis results (i.e. dispersion, AIC, and AUC), it is evident that spectral acceleration at the fundamental period continues to outperform other spectral acceleration IMs. However, in contrast to previous results—where drift as an EDP showed superior performance over acceleration—the IDA results indicate that acceleration as an EDP may perform better when ground motions are scaled.

The effectiveness of the alternative intensity measures presented in Section 3.2 is assessed using these parameters across different EDPs. A summary of the findings is displayed in the table below.

Table 3.5 Summary of Intensity Measure Performance for Drift and Acceleration as EDPs (IDA-LR)

	Case 1: Drift as an EDP			**Case 2: Acceleration as an EDP**		
IM	Beta	AIC	AUC	Beta	AIC	AUC
PGA	0.28	735.23	1.00	0.30	715.21	1.00
Sa(T1)	0.16	-1816.48	1.00	0.12	-3811.94	1.00
SaAvg (0.1-0.2s)	0.35	1603.39	1.00	0.34	1105.04	0.99
SaAvg (0.1-0.4s)	0.41	2352.47	0.99	0.44	2198.88	0.99
SaAvg (0.05-0.15s)	0.27	571.50	1.00	0.24	-393.41	1.00
PGV	0.88	4570.64	0.97	0.89	4186.20	0.97
CAV	1.10	4992.07	0.96	1.07	4520.45	0.96

SCAV	1.14	4969.08	0.96	1.11	4493.81	0.96
SI	1.08	4970.14	0.96	1.10	4609.89	0.96
HI	1.68	5602.42	0.93	1.69	5208.20	0.91
AI	1.21	3614.86	0.99	1.19	3146.88	0.98
HD	/	/	/	/	/	/
TD	/	/	/	/	/	/
RE	0.92	2500.79	0.99	0.74	1170.42	0.99
CAD	2.29	5924.57	0.89	2.25	5495.80	0.88
SV	2.29	5924.57	0.89	2.25	5495.80	0.88
Np	/	/	/	/	/	/
EPA	0.46	2752.00	0.99	0.49	2543.70	0.99
PGD	3.37	6187.28	0.84	3.23	5738.33	0.83

The results from Table 3.5 support the conclusions regarding dispersion variation with spectral acceleration, indicating that using acceleration as an EDP generally provides better performance compared to drift. Additionally, Sa(T1) consistently emerges as the optimal choice for reducing uncertainties across both EDPs, making it the preferred intensity measure when minimizing variability is the objective.

3.4.4 Maximum Likelihood Estimation for Incremental Dynamic Analysis (IDA)

Following the application of Maximum Likelihood Estimation (MLE) in the Cloud Method, this section extends the use of MLE to Incremental Dynamic Analysis (IDA), to explore and compare the performance of the selected intensity measure with IDA approach. Figure 3.14 presents the collapse assessment for two different EDPs—Drift and Acceleration—using PGA as the intensity measure. The fragility curves, obtained through MLE, illustrate the probability of collapse as a function of PGA.

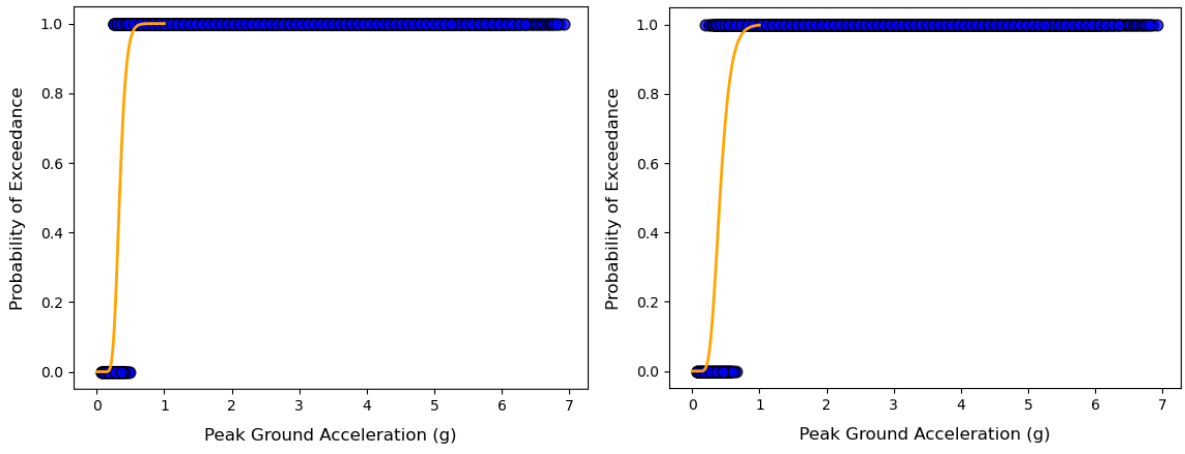

(a) (b)

Figure 3.14 Collapse Assessment with Respect to PGA and Fragility Curve Estimation: (a) Drift as the EDP, (b) Acceleration as the EDP (IDA-MLH)

In a similar manner to the previous section, the fragility parameter (dispersion) was calculated with respect to different spectral accelerations Sa(T) at various structural periods, along with the propagation of uncertainties to provide comprehensive results, as shown in Figure 3.15. Once again, the Sa(T1)

emerges as the optimal intensity measure, demonstrating the strongest correlation. Additionally, a lower discrepancy is observed between the dispersions for EDPs (drift and acceleration) in the IDA approach compared to the Cloud approach.

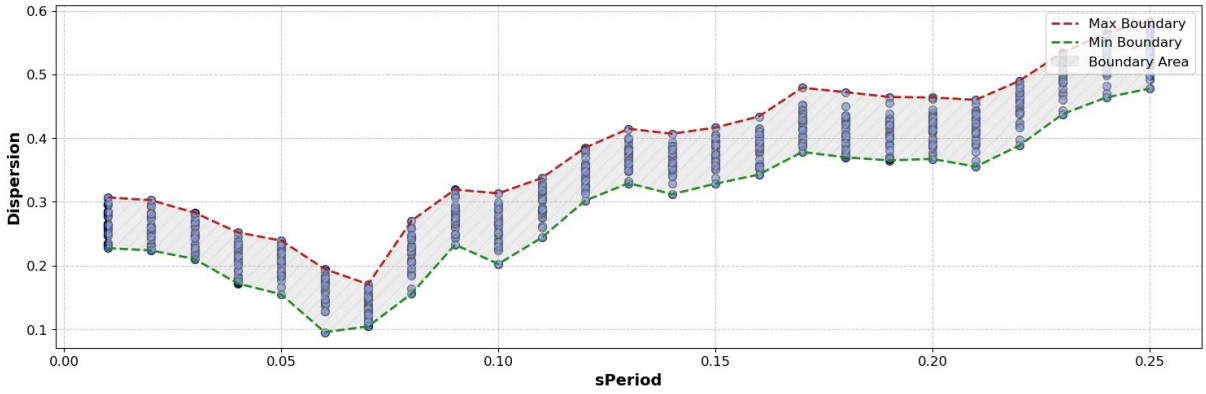

(a)

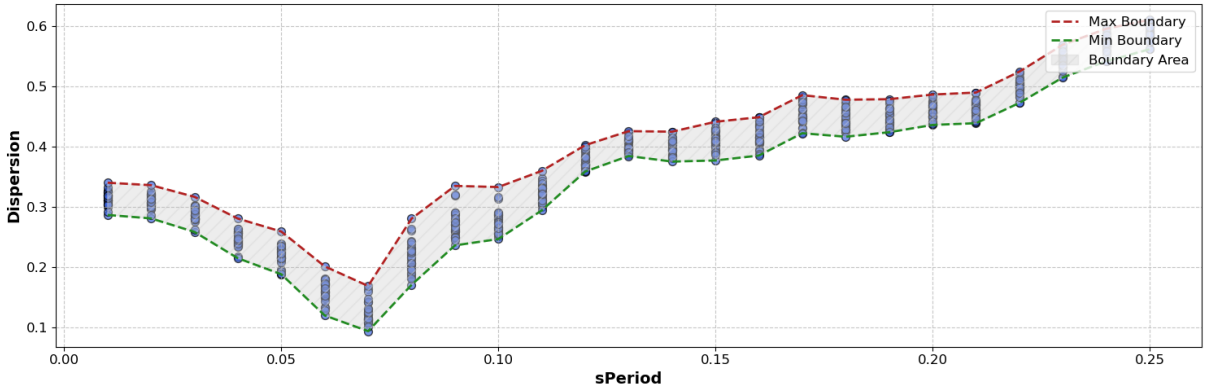

(b)

Figure 3.15 Variation of Dispersion with Respect to Spectral Acceleration at Different Periods: (a) Using Drift as EDP, (b) Using Acceleration as EDP (IDA-MLH)

Table 3.6 Summary of Intensity Measure Performance for Drift and Acceleration as EDPs (IDA-MLH)

	Case 1: Drift as an EDP	Case 2: Acceleration as an EDP
IM	Beta	Beta
PGA	0.26	0.30
Sa(T1)	0.14	0.11
SaAvg (0.1-0.2s)	0.34	0.34
SaAvg (0.1-0.4s)	0.37	0.42
SaAvg (0.05-0.15s)	0.25	0.24
PGV	0.65	0.67
CAV	0.80	0.80
SCAV	0.89	0.88
SI	0.75	0.78
HI	/	/

AI	1.02	1.03
HD	/	/
TD	/	/
RE	0.82	0.70
CAD	1.49	1.53
SV	1.49	/
Np	/	/
EPA	0.41	0.45
PGD	2.11	2.14

The results in Table 3.6 continue to support previous findings, showing that Sa(T1) is the best choice when it comes to minimizing variability across both EDPs (drift and acceleration). With the lowest Beta values in both cases, Sa(T1) proves effective in reducing uncertainty, making it a consistently reliable intensity measure. This table also shows a slight advantage for using acceleration as the EDP, particularly in terms of minimizing variability. Additionally, although the IDA approach is more computationally intensive than the Cloud approach, the dispersion results for different intensity measures are notably lower in IDA analysis.

The fragility comparison in the case of the IDA approach between LR and Maximum Likelihood is shown in the following figure.

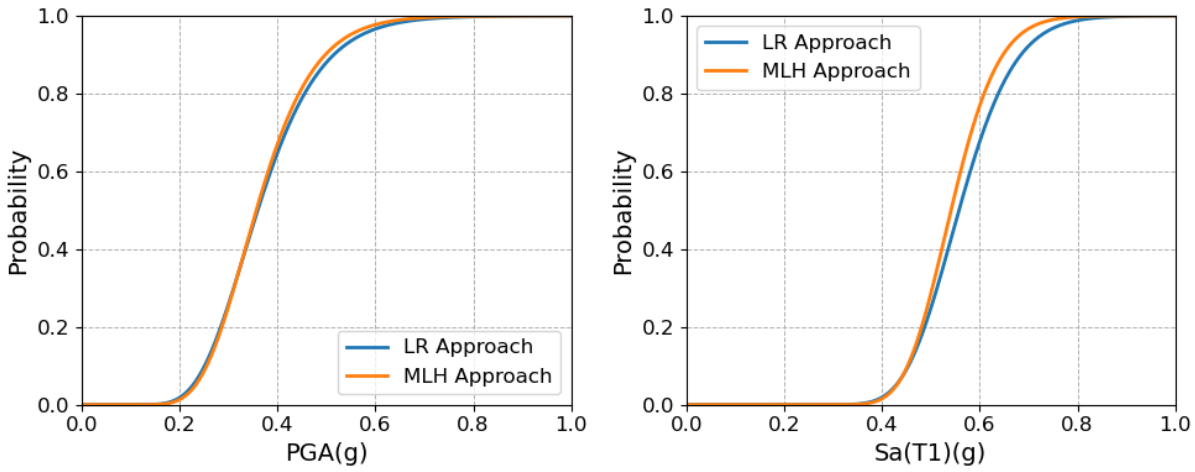

Figure 3.16 Fragility Comparison Based on Cloud LR and MLH Approaches: (a) PGA as Intensity Measure (IM), (b) Sa(T1) as Intensity Measure (IM) (IDA MLH)

3.5 Seismic Fragility Analysis for High-Damage States Based on Scalar IM

Previous studies indicated that selecting spectral acceleration at the fundamental period can be an optimal intensity measure for reducing response uncertainties compared to other intensity measures. Additionally, the findings suggested that, when using a Cloud approach, drift as an engineering demand parameter (EDP) result in lower dispersion. However, when scaling of records is introduced, using acceleration as the EDP may yield slightly lower dispersion than drift.

It is important to note that the 3.4 results focused solely on linear responses. Therefore, in this section, the performance of the intensity measure selected in Section 3.2 is further evaluated. Unlike the previous Cloud analysis, which was restricted to the linear response case, this section exclusively presents the IDA approach using Maximum Likelihood Estimation, as the Linear Regression method assumes a constant dispersion across the intensity measure (IM) levels of interest.

3.5.1 Maximum Likelihood Estimation for Incremental Dynamic Analysis (IDA)

After scaling the ground motions to achieve an extensive nonlinear response range, the threshold for estimating the fragility parameter was set within this nonlinear range. For evaluation purposes, different thresholds at various stages of nonlinearity were considered, with a representative case shown here.

Figure 3.17 illustrates a comparison of fragility curves for two Engineering Demand Parameters (EDPs): Drift (Figure a) and Acceleration (Figure b) in the context of nonlinear response, analyzed using the IDA-MLH (Incremental Dynamic Analysis with Maximum Likelihood Estimation). It appears that higher dispersion is associated with the Acceleration as an EDP (Figure b) compared to Drift (Figure a) in the nonlinear response range. This suggests that using acceleration as the EDP at nonlinear response levels introduces greater variability in the collapse assessment.

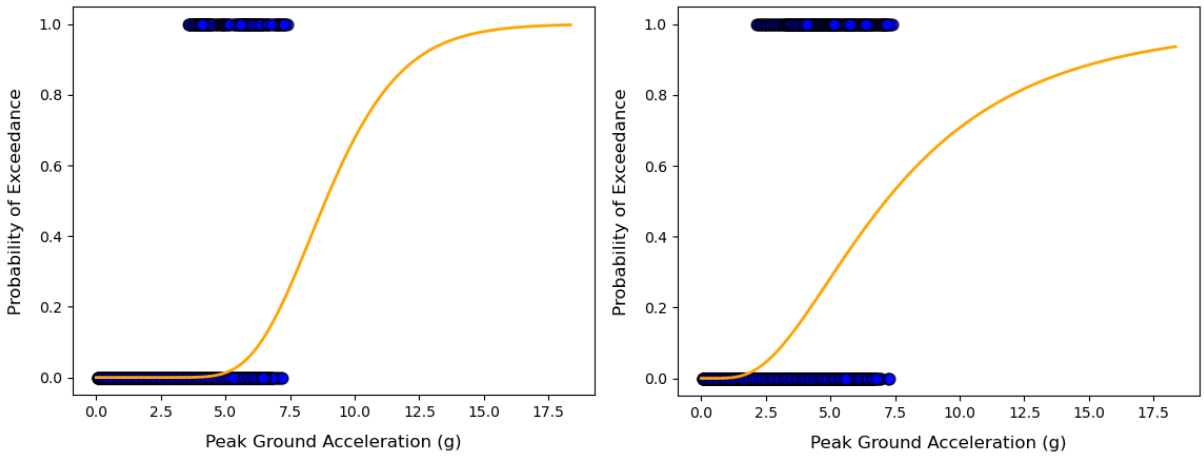

(a) (b)

Figure 3.17 Collapse Assessment with Respect to PGA and Fragility Curve Estimation for Nonlinear Response: (a) Using Drift as the EDP, (b) Using Acceleration as the EDP (IDA-MLH)

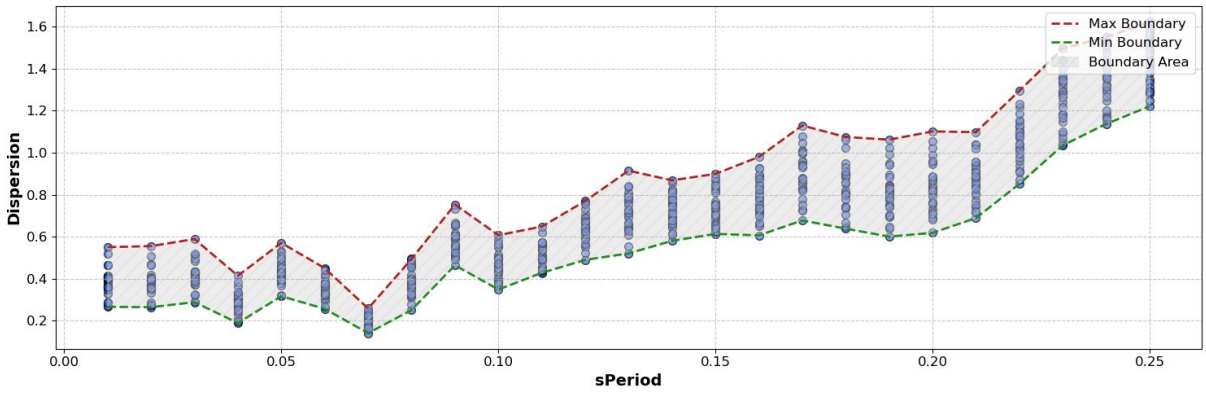

(a)

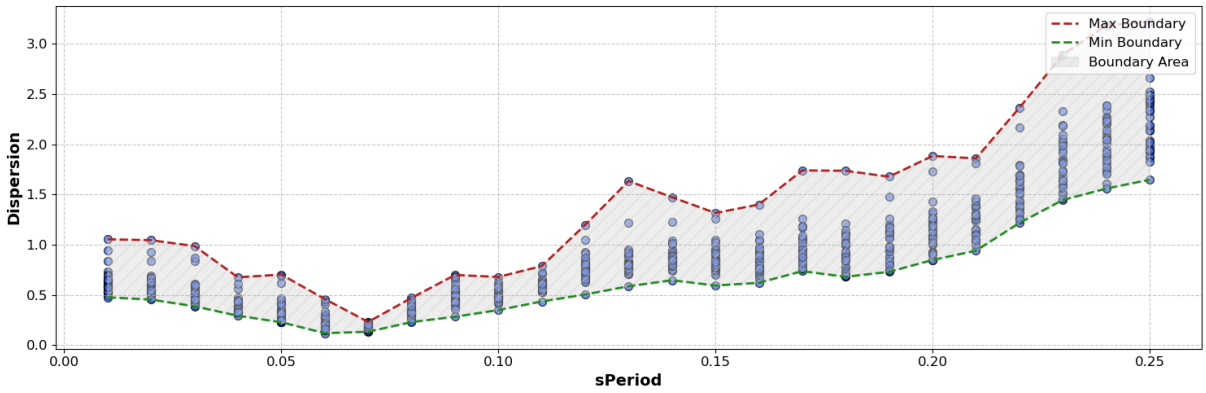

(b)

Figure 3.18 Variation of Dispersion with Respect to Spectral Acceleration at Different Periods of the non-linear response: (a) Using Drift as EDP, (b) Using Acceleration as EDP

During the evaluation of dispersion variation with respect to spectral acceleration at different periods, a recurring non-convergence issue was observed in the nonlinear case, unlike the linear case. This issue is mainly due to data scarcity around the parameter of interest in the optimization process. However, as shown in Figure 3.18, greater variation in dispersion is expected when uncertainty analysis is conducted at a single spectral acceleration, in contrast to the linear response case, where variation was much lower. The figure also indicates that using spectral acceleration at the fundamental period still results in the lowest dispersion. Additionally, selecting drift as the EDP significantly reduces dispersion in the fragility curve.

The performance of the alternative intensity measures discussed in Section 3.2 is evaluated across different EDPs using these parameters. The table below presents a summary of the findings.

Table 3.7 Summary of Intensity Measure Performance for Drift and Acceleration as EDPs for nonlinear structural behavior

	Case 1: Drift as an EDP	**Case 2: Acceleration as an EDP**
IM	Beta	Beta
PGA	0.39	0.63
Sa(T1)	0.18	0.19
SaAvg (0.1-0.2s)	0.60	0.64
SaAvg (0.1-0.4s)	0.72	1.02
SaAvg (0.05-0.15s)	0.41	0.38
PGV	2.10	2.73
CAV	2.69	2.70
SCAV	2.78	2.86
SI	2.74	3.82
HI	/	/
AI	2.59	2.82
HD	/	/
TD	/	/
RE	1.62	0.83
CAD	/	/

SV	/	/
Np	/	/
EPA	0.86	1.21
PGD	/	/

Table 3.7 shows that dispersion values from nonlinear behavior are generally higher compared to the linear case, primarily due to the complexity of the structure's nonlinear (material) response. Nevertheless, in both linear and nonlinear cases, spectral acceleration at the structure's fundamental period remains the optimal choice among the intensity measures. Regarding EDPs, drift appears to perform slightly better than acceleration when using spectral acceleration as the IM. A more notable difference is observed with other IMs; for example, with PGA, dispersion values are 0.39 for drift and 0.63 for acceleration, indicating a clear advantage for drift in this case.

3.6 Seismic Fragility Analysis for Low-Damage States Based on Vector IM

The purpose of extending the scalar fragility curve to a vector fragility approach is to reduce uncertainties in the response [41–45], specifically by minimizing dispersion.

In this section, an optimal combination of intensity measures from a total of 171 combinations, as introduced in Section 3.2, is explored. Two approaches—Multiple Linear Regression (MLR) and Maximum Likelihood Estimation (MLH)—are applied to vector intensity measures, similar to the scalar IM approach, using two different Engineering Demand Parameters (EDPs): drift and acceleration, based on a linear structural response. The dispersion resulting from this optimal combination is then compared with that of the optimal scalar intensity measure.

3.6.1 Cloud - Multiple Linear Regression (MLR)

Multiple linear regression is a statistical method in which a dependent variable can be expressed through multiple independent variables [46–48]. The equation for linear regression represents the relationship between earthquake intensities (IMs) and the Engineering Demand Parameters (EDPs), For two independent variables, this relationship can, for example, be illustrated as following:

$$\ln \mathrm{EDP} = \mathrm{a} + b \ln \mathrm{im}_1 + \mathrm{c} \ln \mathrm{im}_2 + \mathrm{e} \qquad (Eq.7)$$

where:

- a,b and c are coefficients to be estimated from the multiple linear regression.
- e is a zero-mean random variable representing the remaining variability in ln EDP given IM.
- IM1 and IM2 are the intensity measures.

Assuming ln EDP is normally distributed, then the probability of exceeding an EDP level y given IM = (im1, im2) can be estimated as:

$$G_{EDP|IM}(y|im) = 1 - \Phi\left(\frac{\ln y - (\hat{a} + \hat{b} \ln \mathrm{im}_1 + \hat{c} \ln \mathrm{im}_2)}{\hat{\sigma}_e}\right) \qquad (Eq.8)$$

Where $\hat{a}$, $\hat{b}$, $\hat{c}$ are the regression estimates of the coefficients a,b and c. $\Phi(.)$ is the Cumulative Distribution Function (CDF) of the standard Gaussian distribution and $\hat{\sigma}_e$ is the standard deviation of the residuals, which could be estimated by the following:

$$\hat{\sigma}_e = \sqrt{\frac{\sum_i^n (\ln EDP - \ln \widehat{EDP})^2}{n-2}} \qquad (Eq.9)$$

Where n is the number of records used in the regression.

$G_{EDP|IM}(y|im)$ is the complementary cumulative distribution function (CCDF), By plotting this function against various IM levels, the fragility curve is obtained.

According to this definition, Figure 3.19-(a) provides an example illustrating the relationship between the drift response of the DGB simplified model and the two intensity measures, Sa(T1) and SaAvg (0.05-0.15s). Figure 3.19-(b) illustrate the Iso lines of the surface fragility obtained after the threshold definition using the MLR.

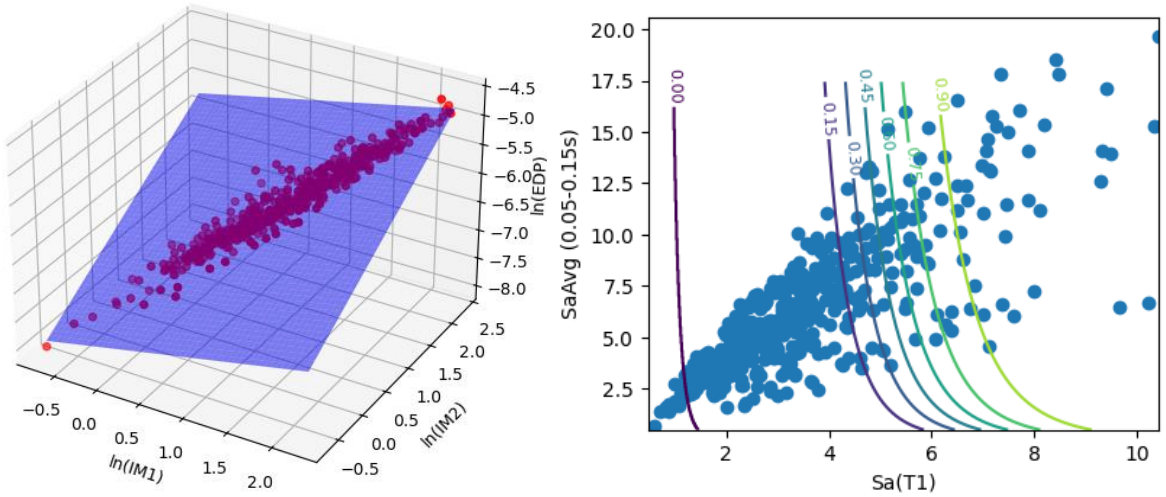

(a) (b)

Figure 3.19 (a) Logarithmic Relationship Between Structural Response and Intensity Measures Using MLR (b) Fragility surface Iso lines and regression model

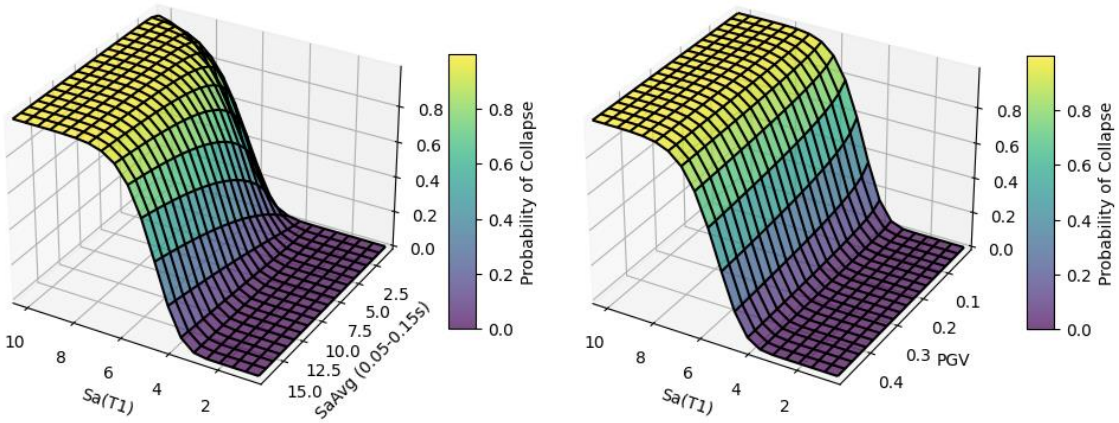

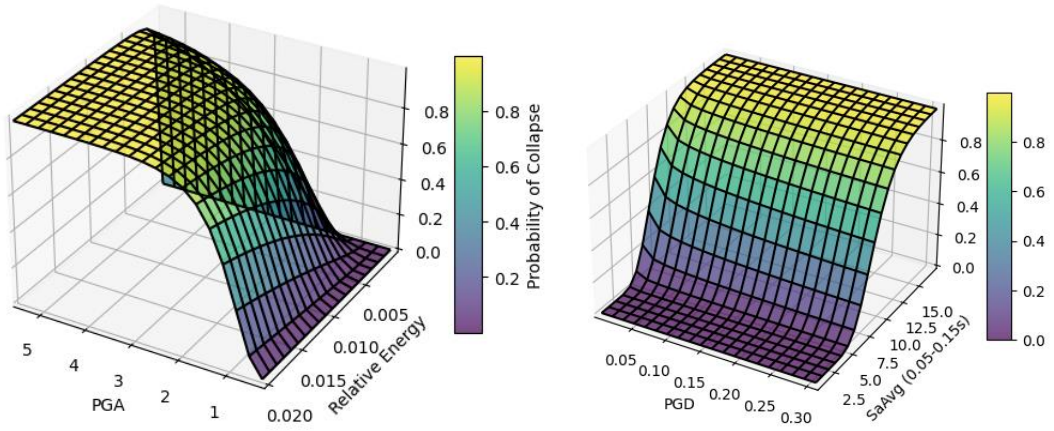

Figure 3.20 3D Fragility Surfaces: Probability of Collapse as a Function of Various Seismic Intensity Measures

Taking into account the chosen intensity measures, the optimal combination was determined based on the lowest observed dispersion. With 19 intensity measures selected, this resulted in 171 possible combinations, calculated using C_2^{19}. After applying the multiple linear regression approach to these combinations, the resulting heatmap, shown below, illustrates the dispersion values for each combination:

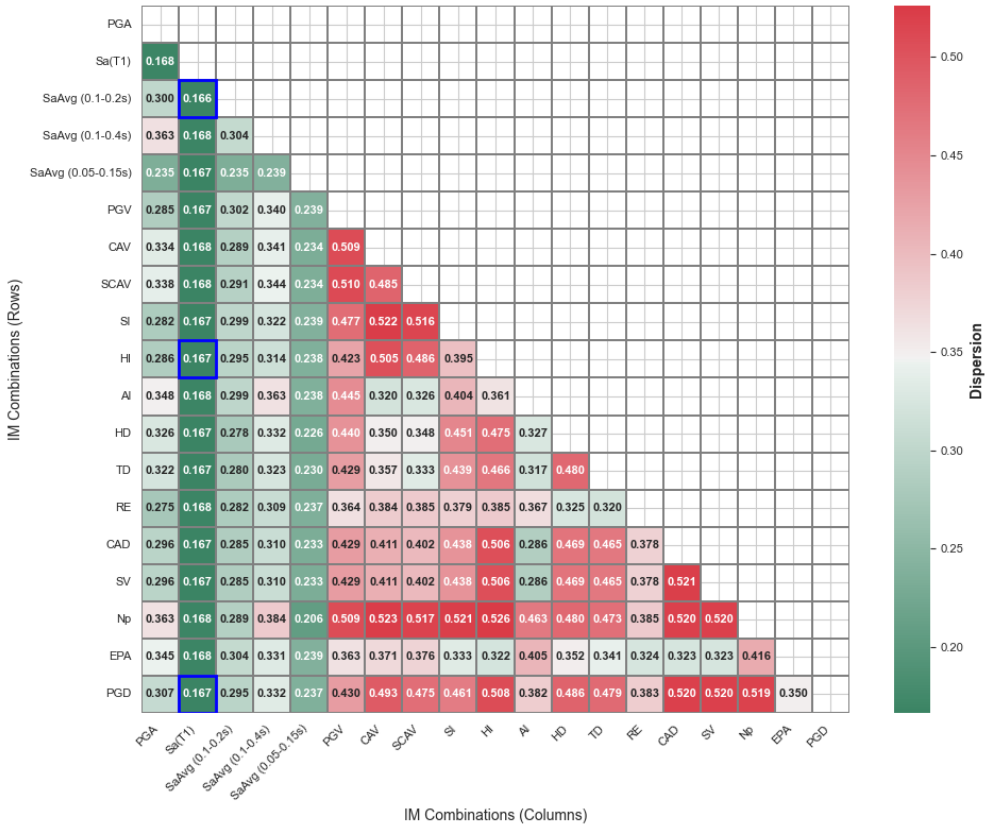

(a)

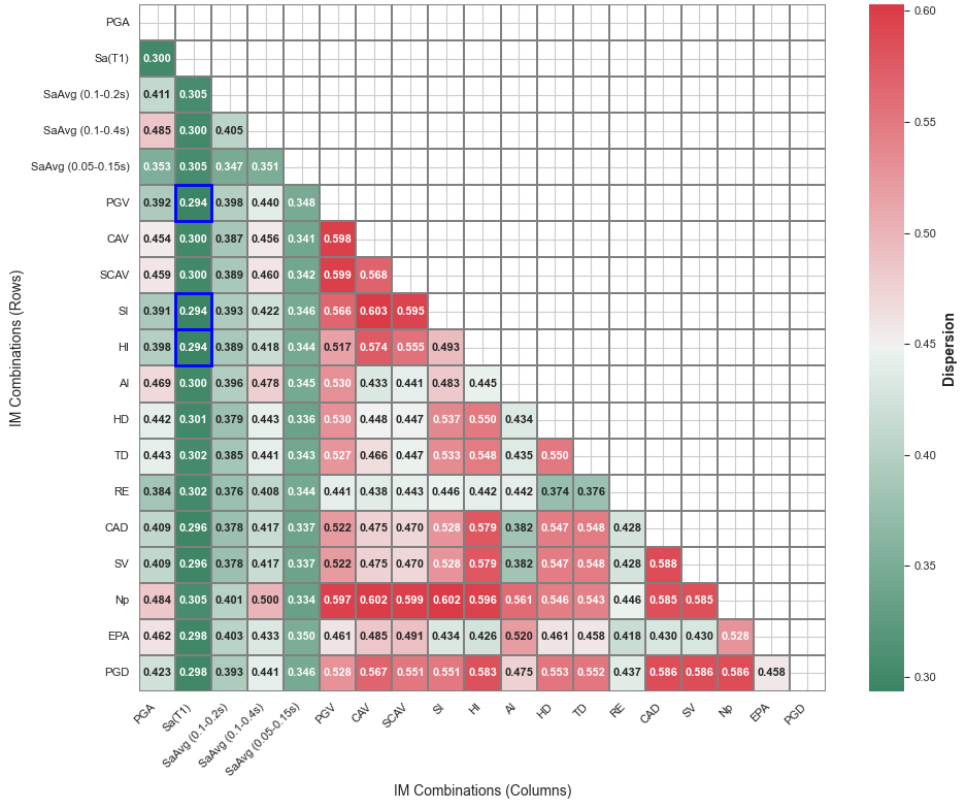

(b)

Figure 3.21 Dispersion Heatmap for Optimizing IM Combinations Vector-MLR Cloud: (a) Drift as an EDP (b) Acceleration as an EDP

The heatmap in Figure 3.21 demonstrates that Sa(T1) and SaAvg (0.05–0.15s) consistently perform best in minimizing dispersion, with a value of 0.166. Following these, combinations like (Sa(T1), PGD) and (Sa(T1), HI) also show relatively low dispersion, though slightly higher. In contrast, the remaining intensity measures such as CAV, SCAV, and CAD show high dispersion values and may not be ideal for applications requiring low uncertainty. Additionally, the results from the vector analysis in terms of EDP selection align closely with those from the scalar section. The dispersion is lower when drift is used as the EDP compared to when acceleration is selected as the EDP.

For comparison between vector and scalar fragility, these results indicate that adding an extra intensity measure can slightly reduce dispersion. As noted in Section 3.4.1, the optimal scalar intensity measure, Sa(T1), had a dispersion of 0.17, while the optimal vector case achieved a slightly lower dispersion of 0.166. This comparison is further illustrated in Figure 3.22, which shows fragility plots for both a single IM and a vector IM case. In Figure 3.22, (a) presents a vector case where PGA is combined with SaAvg (0.1–0.2s), and (b) shows the optimal IM combination identified in the heatmap compared to Sa(T1) from the single intensity measure case.

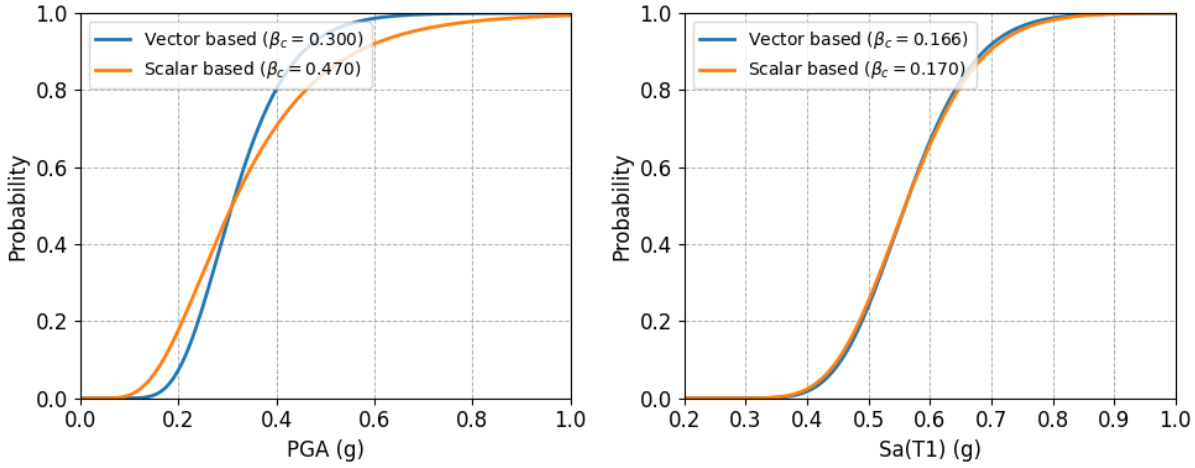

(a) (b)

Figure 3.22 Fragility Curve Comparison: (a) Vector-Based and Scalar-Based for PGA, (b) Vector-Based and Scalar-Based for Sa(T1)

3.6.2 Cloud - Maximum Likelihood Estimation (MLH)

The methodology for vector fragility analysis using maximum likelihood, as originally presented in [49] , aims to reduce dispersion by combining two or more intensity measures (IMs). The proposed damage probability function is expressed as follows:

$$P_f(im_1, im_2) = P(ds \geq DS | IM_1 = im_1, IM_2 = im_2) = \frac{1}{2}[1 + erf(c_1 + c_2 \log im_1 + c_3 \log im_2)] \quad \text{(Eq. 10)}$$

Where erf is the error function and c_1, c_2 and c_3 are coefficients to be estimated.

The new intensity measure (IM), which combines the two selected IMs, can be expressed in the following format:

$$im_v = im_1^{\frac{c_2}{c_2+c_3}} \cdot im_2^{\frac{c_3}{c_2+c_3}} \quad \text{(Eq. 11)}$$

From this, the damage probability function can be expressed in the following format:

$$P_f(im_1, im_2) = P(ds \geq DS | IM_1 = im_1, IM_2 = im_2) = \frac{1}{2}[1 + erf(c_1 + c_2 \log im_1 + c_3 \log im_2)] =$$
$$\frac{1}{2}\left[1 + erf\left(\frac{\frac{c_1}{c_2+c_3} + \ln im_1^{\frac{c_2}{c_2+c_3}} + \ln im_2^{\frac{c_3}{c_2+c_3}}}{\frac{1}{c_2+c_3}}\right)\right] = \frac{1}{2}\left[1 + erf\left(\frac{\ln im_v - \ln \alpha_v}{\beta_v \sqrt{2}}\right)\right] \quad \text{(Eq. 12)}$$

Where α_v and β_v are the fragility parameter, could be estimated using the following:

$$\alpha_v = \exp\left(\frac{-c_1}{c_2+c_3}\right) \quad \text{(Eq. 13)}$$

$$\beta_v = \frac{1}{(c_2+c_3)\sqrt{2}} \quad \text{(Eq. 14)}$$

The C coefficients can be estimated using the maximum likelihood function, as shown below:

$$L(\alpha_v, \beta_v) = \prod_{i=1}^{n} [P_f(im_i, \alpha_v, \beta_v)]^{y_i} [1 - P_f(im_i, \alpha_v, \beta_v)]^{1-y_i} \quad \text{(Eq. 15)}$$

Following this definition, the vector fragility surface is visualized in the 3D plots below. These plots

illustrate the probability of collapse as a function of two selected intensity measures (IMs).

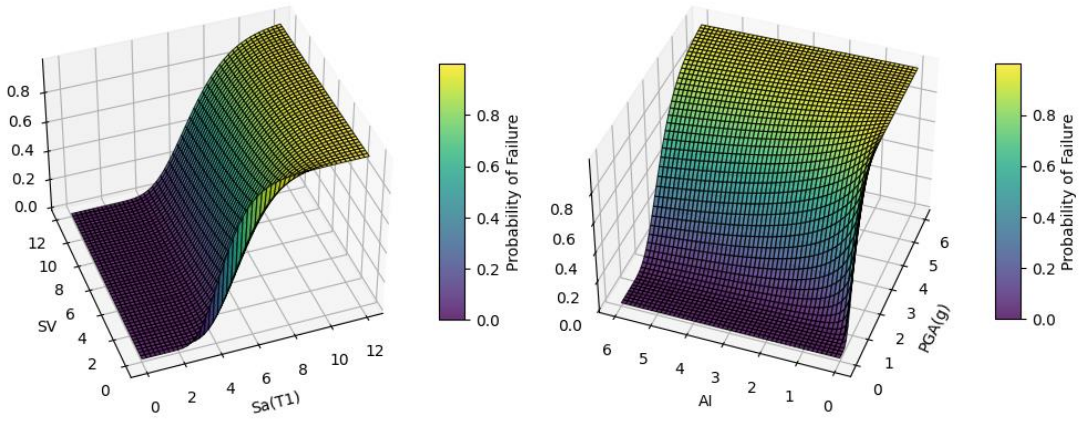

(a) (b)

Figure 3.23 Fragility Surface using vector IMs: (a) Spectral Acceleration and Squared Velocity (b) Aria Intensity and Peak Ground Acceleration

Similar to the previous section, a total of 171 combinations were evaluated based on the resulting dispersion from the Vector-MLH fragility analysis for both Drift and Acceleration as EDPs. The results are visualized in the following heatmaps.

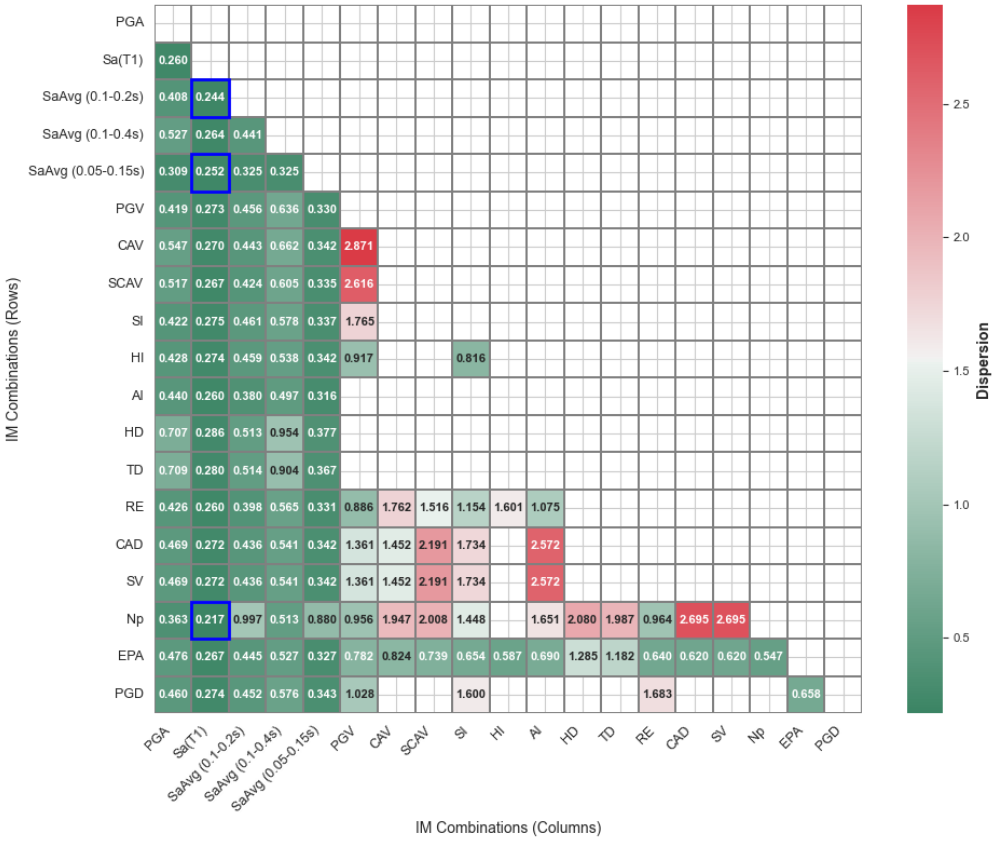

(a)

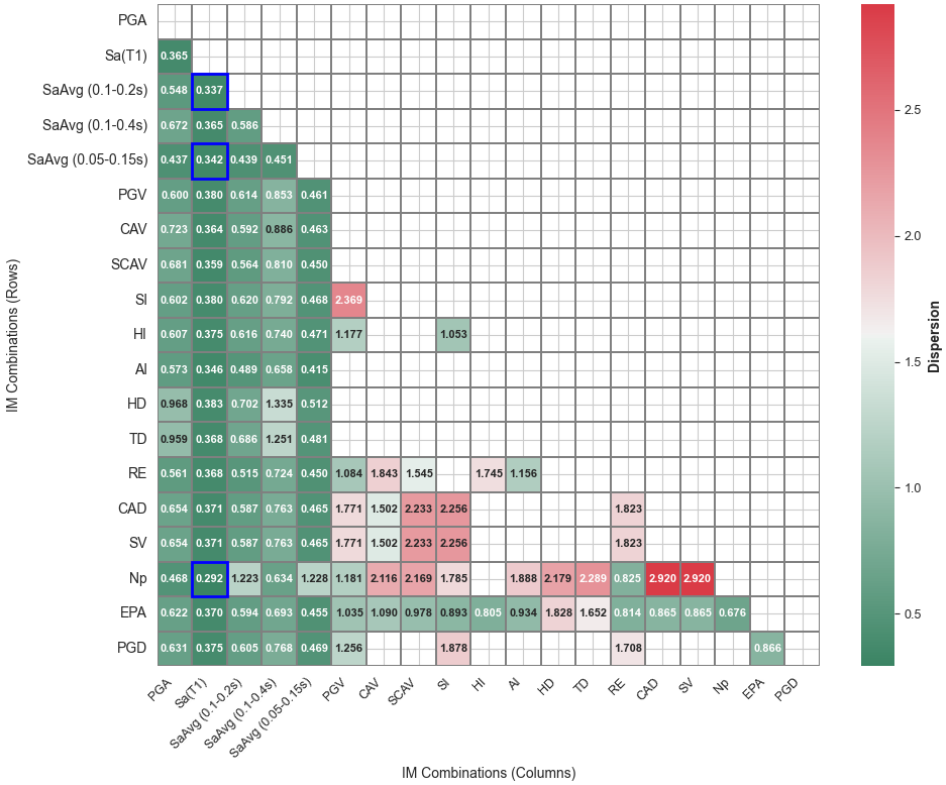

(b)

Figure 3.24 Dispersion Heatmap for Optimizing IM Combinations Vector-MLH Cloud: (a) Drift as an EDP (b) Acceleration as an EDP

The results from the V-Cloud MLH analysis indicate that using drift as the engineering demand parameter leads to lower uncertainties in the response. This is clearly observed in the analysis, where the optimal dispersion for the drift case is 0.22, compared to 0.3 for the acceleration case. Furthermore, consistent with findings from the scalar analysis, incorporating Sa(T1) as one of the intensity measures (IM1, IM2) generally results in reduced dispersion. In this study, the combination (Sa(T1), Np) was identified as the optimal pairing for both EDPs.

When comparing these findings with the scalar analysis results, it appears that the vector-based approach achieves a lower dispersion. For the Vector-Drift-Case, an optimal dispersion of 0.22 was obtained, compared to 0.27 for the scalar approach, reflecting a reduction of approximately 20%. In the Vector-Acceleration-Case, this difference is slightly greater, at around 23%. To illustrate this, the comparison between the fragility curve of the scalar case and a slice of the fragility surface for the vector case is presented below for PGA and Sa(T1).

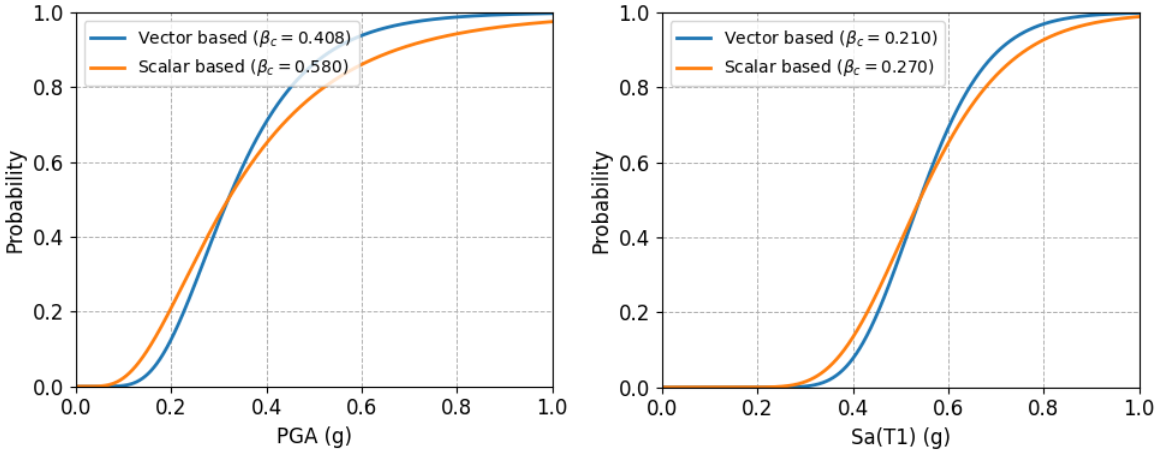

(a) (b)

Figure 3.25 Fragility Curve Comparison using Cloud MLH approach: (a) Vector-Based and Scalar-Based for PGA, (b) Vector-Based and Scalar-Based for Sa(T1)

3.6.3 Incremental Dynamic Analysis - Multiple Linear Regression (MLR)

For the sake of comparison, an incremental analysis on a vector scale was also performed. By employing Multiple Linear Regression (MLR), the logarithmic relationship between the Engineering Demand Parameter (EDP) and the two intensity measures was established. The figure below illustrates this relationship, along with a plot of the structural response and the corresponding iso-probability lines derived from the vector-valued fragility function.

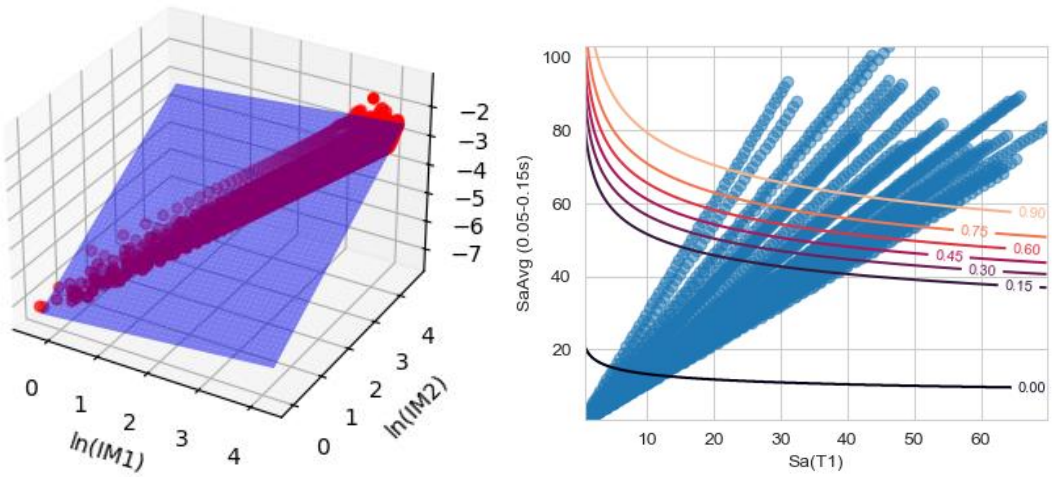

(a) (b)

Figure 3.26 (a) Logarithmic Relationship Between Structural Response and Intensity Measures Using MLR (b) Iso-probability lines corresponding to some examples of vector-valued fragility function

Following the selection of Intensity Measures (IMs), Multiple Linear Regression (MLR) was utilized to identify the combination of IMs that minimizes dispersion. The resulting analyses for drift and acceleration, considered as Engineering Demand Parameters (EDPs), are depicted in the two heatmaps below:

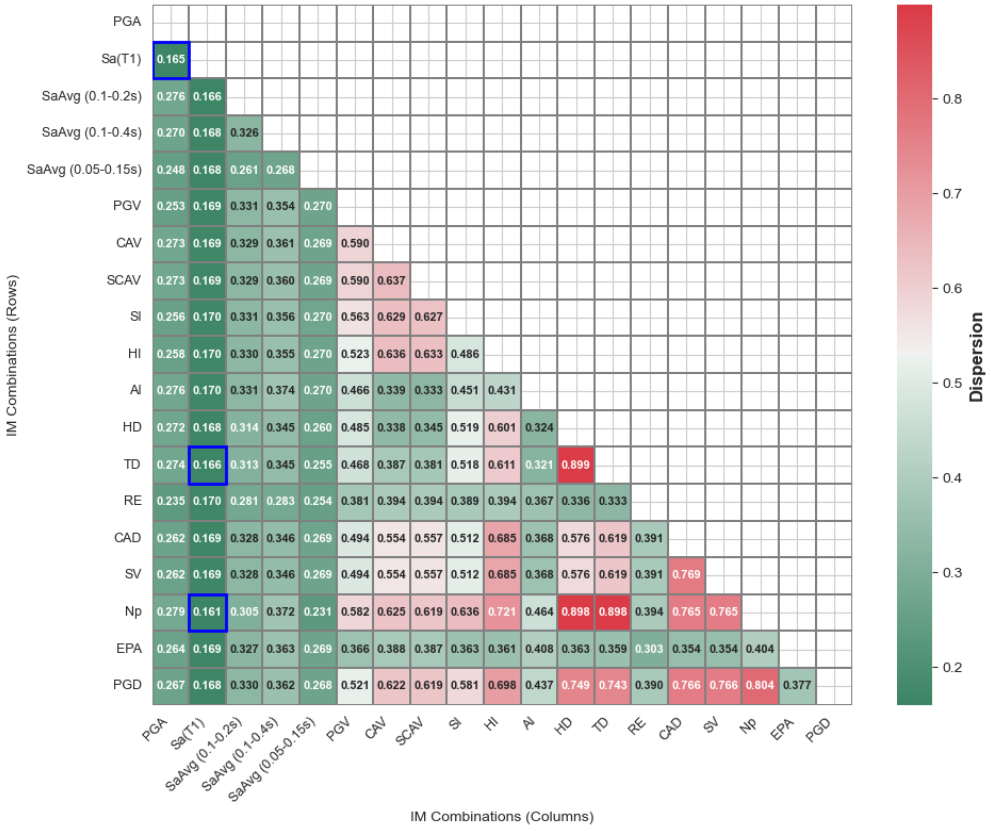

(a)

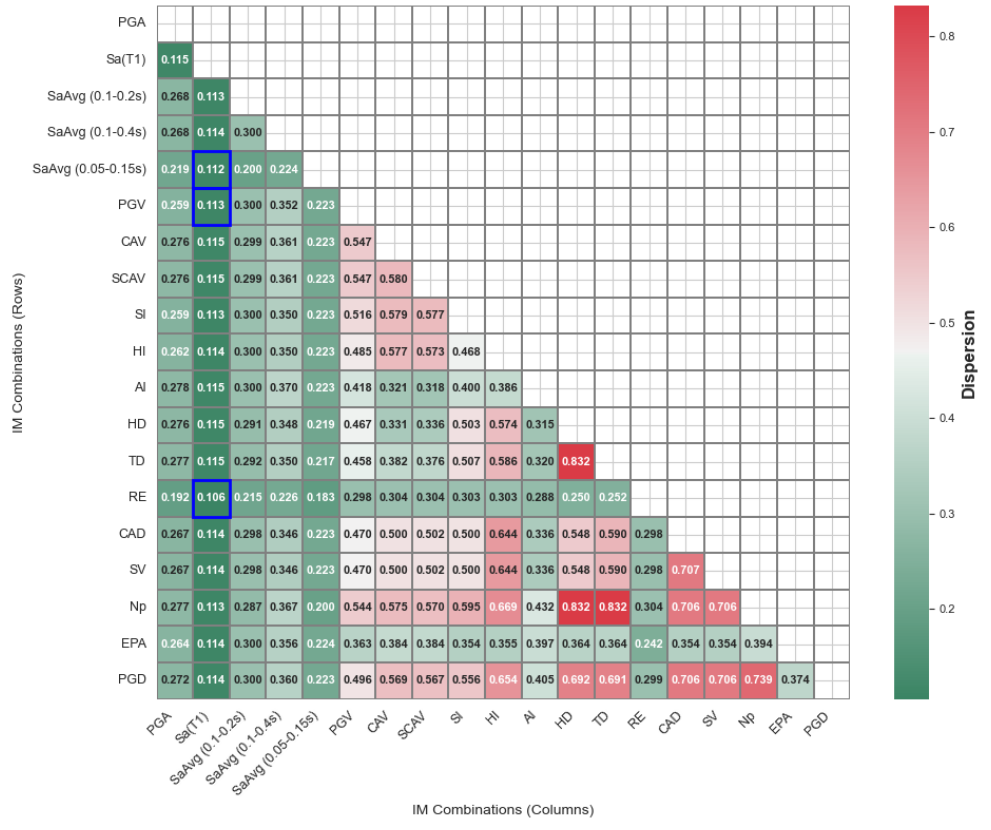

(b)

Figure 3.27 Dispersion Heatmap for Optimizing IM Combinations Vector-MLR IDA: (a) Drift as an EDP (b) Acceleration as an EDP

The comparison of IDA-Vector drift results with Cloud-Vector drift results reveals similar dispersion levels. However, a notable reduction in dispersion is observed for acceleration in the case of IDA-Vector. This stands in contrast to the results from the previous section, where the selection of EDPs showed minimal dispersion for drift-based EDPs. For the IDA approach, acceleration-based EDPs exhibit the lowest dispersion. This outcome may be attributed to the methodology employed in the IDA approach, which incrementally increases acceleration until the desired deformation is achieved, resulting in a stronger correlation. Additionally, the dynamic characteristics of the case study, particularly its high-frequency range, further contribute to this observation.

Moreover, selecting spectral acceleration at the fundamental period as one of the intensity measures helps reduce the uncertainties in the response. This result is consistently observed for both case studies—drift and acceleration.

As an example, the comparison between vector-based and scalar intensity measure fragility for Peak Ground Acceleration (PGA) is illustrated in the figure below.

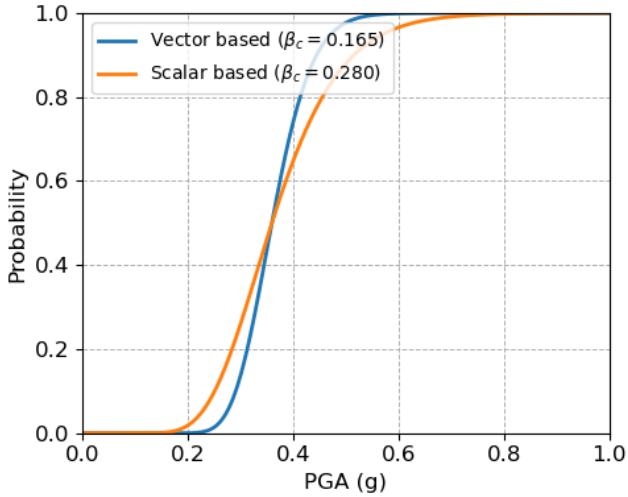

Figure 3.28 Fragility Curve Comparison using IDA MLR approach Vector-Based and Scalar-Based for PGA

3.6.4 Incremental Dynamic Analysis - Maximum Likelihood Estimation (MLH)

The formulation presented in Section 3.6.2 was applied to the responses obtained using the IDA methodology. The fragility parameter (dispersion) was calculated for the previously discussed IM combinations, and the results are illustrated in the two heatmaps below.

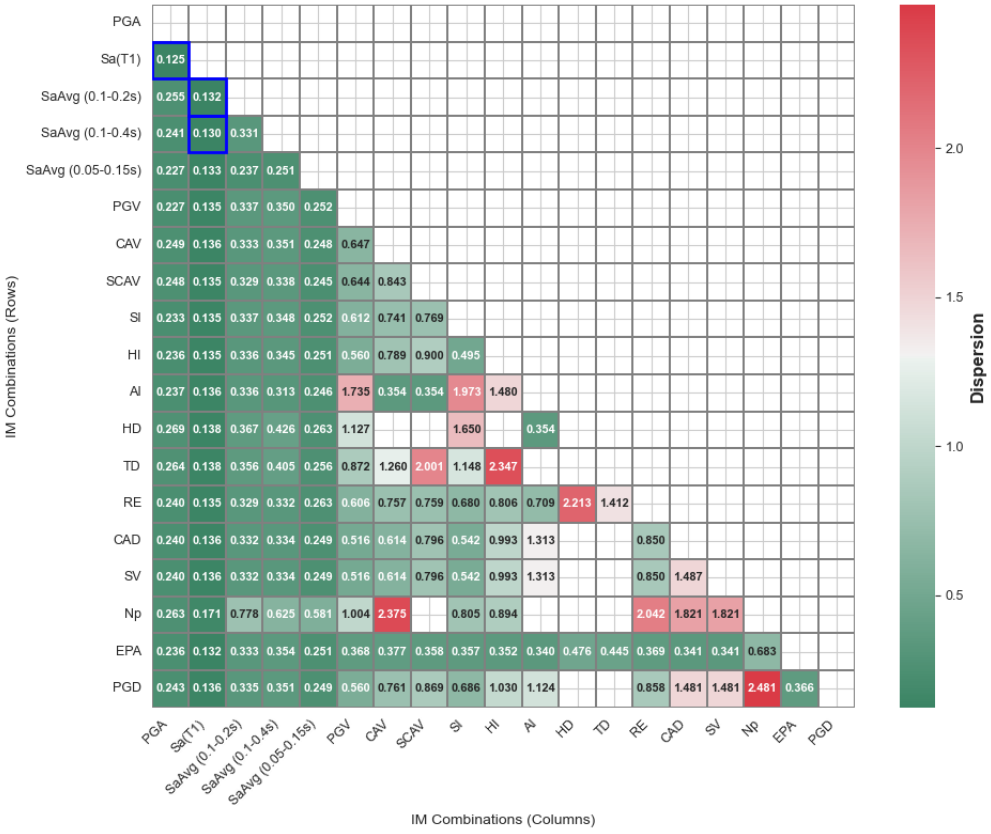

(a)

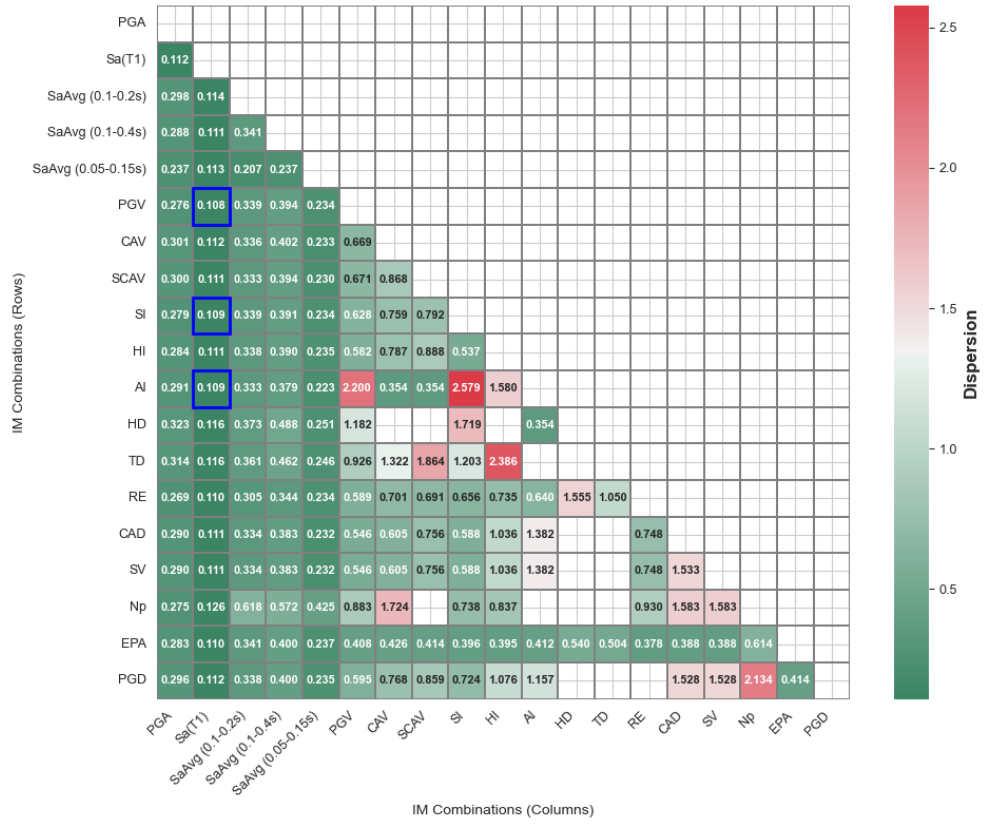

(b)

Figure 3.29 Dispersion Heatmap for Optimizing IM Combinations Vector-MLH IDA: (a) Drift as an EDP (b) Acceleration as an EDP

The results from all cases of structural linear response (scalar and vector) align consistently, leading to the conclusion that selecting the spectral acceleration at the fundamental period effectively reduces dispersion. Regarding the selection of EDPs, employing the Cloud approach suggests that drift yields lower dispersion, whereas in the case of IDA, acceleration demonstrates the lowest uncertainties in the response.

As the final example in this section, the comparison between vector and scalar intensity measures for IDA using the maximum likelihood approach is illustrated below.

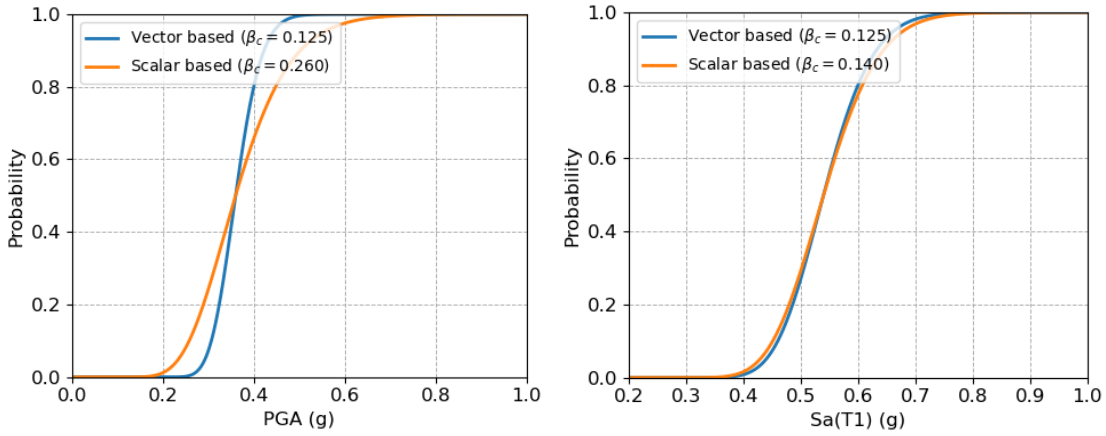

(a) (b)

Figure 3.30 Fragility Curve Comparison using IDA MLH approach: (a) Vector-Based and Scalar-Based for PGA, (b) Vector-Based and Scalar-Based for Sa(T1)

3.7 Seismic Fragility Analysis for High-Damage States Based on Vector IM

The results from the previous section indicated that selecting spectral acceleration at the fundamental period as one of the intensity measures minimizes the fragility parameter (dispersion). However, this conclusion is specific to the case study involving linear structural response. Therefore, this section aims to evaluate the validity of this conclusion under different conditions.

As previously mentioned, the responses obtained from the Cloud approach (without ground motion scaling) correspond to linear structural responses. Consequently, this section focuses on results derived using the IDA approach, employing Maximum Likelihood (MLH) method along with two different EDPs: displacement and acceleration.

3.7.1 Incremental Dynamic Analysis - Maximum Likelihood Estimation (MLH)

After scaling 30 ground motions to achieve the desired deformation, a limit state incorporating structural nonlinearity was selected. Based on the definition of Maximum Likelihood (MLH) for vector fragility (outlined in Section 3.6.2), the following 3D fragility plot was generated, illustrating the relationship with respect to different intensity measures.

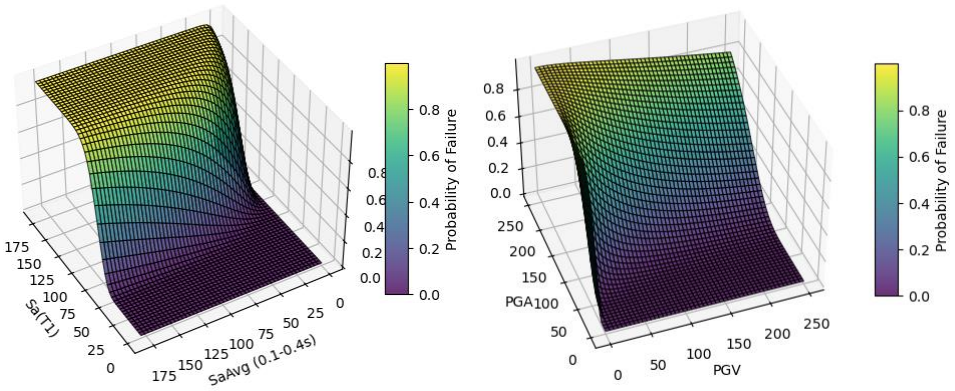

(a) (b)

Figure 3.31 Fragility Surface using vector IMs: (a) Spectral Acceleration and average spectra (0.1-0.4s) (b) Peak Ground Velocity and Peak Ground Acceleration

To further assess the selected Intensity Measures (IMs) for the nonlinear behavior, Maximum Likelihood Estimator (MLH) was applied to examine various IM combinations, focusing on minimizing the associated dispersion. Heatmaps below illustrate the outcomes for drift and acceleration, which were used as Engineering Demand Parameters (EDPs) in the analysis.

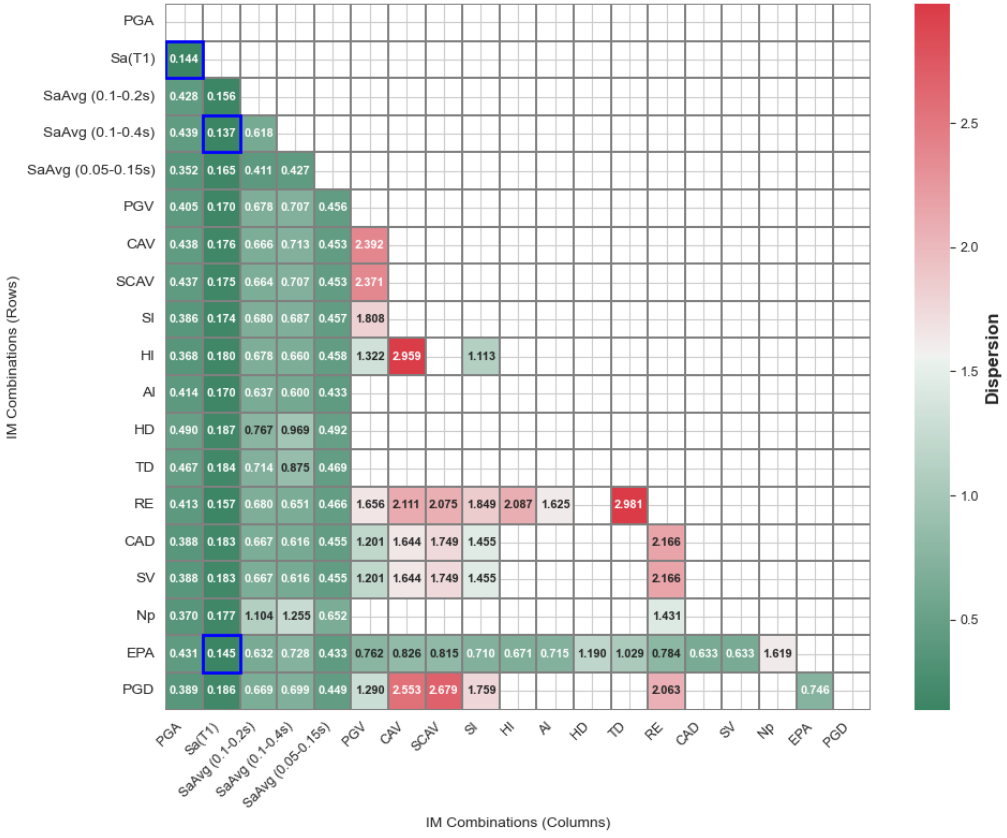

(a)

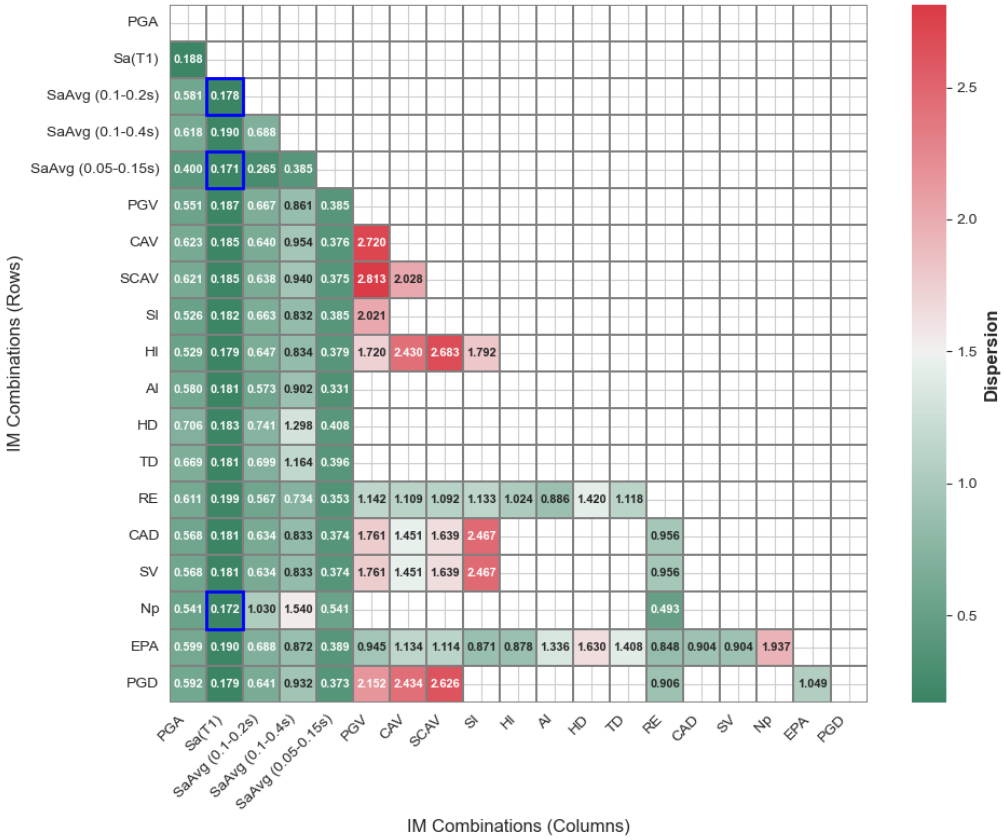

(b)

Figure 3.32 Dispersion Heatmap for Optimizing IM Combinations Vector-MLH Non-Linear Response: (a) Drift as an EDP (b) Acceleration as an EDP

Considering the nonlinearity in the structural response, an increase in dispersion values is expected. This is evident in Figure 3.32, where the dispersion values are compared to those in Section 3.6.4. In the nonlinear analysis, the optimal dispersion for drift is 0.14, compared to 0.12 in the linear case. For acceleration as an engineering demand parameter, the difference in dispersion becomes more noticeable.

The findings from the nonlinear analysis align closely with the conclusions drawn from the linear response analysis. Specifically, selecting Sa(T1) as one of the intensity measures continues to yield a significant reduction in dispersion. A comparative analysis of the nonlinear fragility curves, derived from both scalar and vector approaches using two different intensity measures, is illustrated in the figure below.

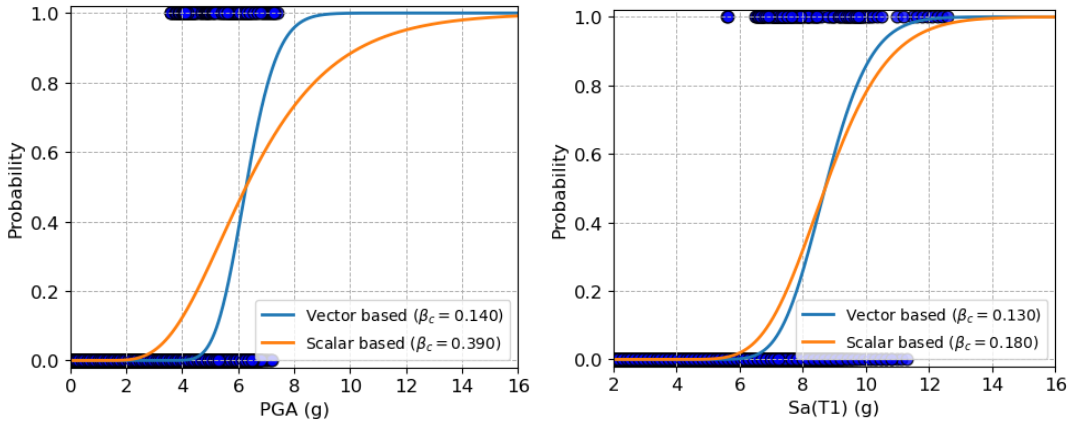

(a) (b)

Figure 3.33 Fragility Curve Comparison using IDA MLH approach for nonlinear response (Case: Drift as EDP): (a) Vector-Based and Scalar-Based for PGA, (b) Vector-Based and Scalar-Based for Sa(T1)

It is worth noting that adding another intensity measure (vector-IM case) results in a slight difference compared to scalar IM when considering linear response. However, for nonlinear response, this difference is expected to be larger. This suggests that applying vector-IM may be more practical when the structure is likely to exhibit significant nonlinear behavior.

4 Conclusions

This report has provided a comprehensive evaluation and comparison of scalar and vector intensity measures (IMs) in fragility analysis, considering both linear and nonlinear structural responses. Within this framework, a simplified model was developed for the Diesel Generator Building of the Zaporizhzhia Nuclear Power Plant (NPP), later validated against the more complex model. The analysis incorporated two fragility methodologies: one using unscaled ground motions (Cloud analysis) and another with scaled ground motions (Incremental Dynamic Analysis, IDA). These approaches were further assessed using Linear Regression and Maximum Likelihood Estimation methods, with drift and acceleration as the engineering demand parameters (EDPs).

The performance of scalar intensity measures was evaluated using three statistical parameters: dispersion (β), Akaike information criterion (AIC), Area under the curve (AUC) to give a solid conclusion. These metrics provided a robust basis for drawing conclusions. The scalar analysis demonstrated that spectral acceleration at the fundamental period Sa(T1) consistently outperformed other intensity measures across all three parameters, for both linear and nonlinear structural responses.

The results from the vector IM analysis indicate that selecting Sa(T1) as one of the intensity measures in the combination leads to low uncertainties in the response across both fragility approaches and for both linear and nonlinear responses. However, the findings also suggest that the vector-IM approach is more effective for nonlinear structural responses. This is attributed to the relatively minor differences observed between vector and scalar IMs in the case of linear structural responses, whereas the benefits of the vector-IM approach become more significant in nonlinear scenarios in case of optimal IM.

Drift as an EDP consistently produced lower dispersion compared to acceleration, aligning with conclusions from both scalar and vector analyses. This highlights drift as a more reliable indicator for fragility assessments.

In summary, this report highlights the critical role of intensity measure selection in fragility analysis, demonstrating the consistent performance of spectral acceleration at the fundamental period, across

both scalar and vector approaches. While scalar IMs provide robust results, the vector-IM approach proves to be particularly advantageous for nonlinear structural responses, offering reduced uncertainties. Additionally, the findings emphasize the reliability of drift as an engineering demand parameter, consistently yielding lower dispersion compared to acceleration.

5 References

[1] M. Korres, V. Alves-Fernandes, I. Zentner (EDF), M. Pilz, Metis Project Deliverable D5.3 "Strategies for response modelling Development of surface ground motions from rockhazard consistent ground motions" (2024).

[2] Asdea, ASDEA software technology, scientific ToolKit for OpenSees, STKO. (2023).

[3] McKenna, F., Fenves, G. L, and Scott, M. H., Open System for Earthquake Engineering Simulation.

[4] I. Hajirasouliha, A. Doostan, A simplified model for seismic response prediction of concentrically braced frames, Advances in Engineering Software 41 (2010) 497–505. https://doi.org/10.1016/j.advengsoft.2009.10.008.

[5] A.M.B. Nafeh, G.J. O'Reilly, Simplified pushover-based seismic risk assessment methodology for existing infilled frame structures, Bull Earthquake Eng 21 (2023) 2337–2368. https://doi.org/10.1007/s10518-022-01600-y.

[6] S. Themelis, PUSHOVER ANALYSIS FOR SEISMIC ASSESSMENT AND DESIGN OF STRUCTURES (2008).

[7] FEMA, Improvement of Nonlinear Static Seismic Analysis Procedures.

[8] J.H. Kim, I.-K. Choi, J.-H. Park, Uncertainty analysis of system fragility for seismic safety evaluation of NPP, Nuclear Engineering and Design 241 (2011) 2570–2579. https://doi.org/10.1016/j.nucengdes.2011.04.031.

[9] EPRI, Seismic Fragility and Seismic Margin Guidance for Seismic Probabilistic Risk Assessments.

[10] M.A. Hariri-Ardebili, S. Sattar, Sensitivity analysis of reinforced concrete structures, National Institute of Standards and Technology (U.S.), Gaithersburg, MD, 2023.

[11] H.D. Nguyen, M. Shin, J.M. LaFave, Optimal intensity measures for probabilistic seismic demand models of steel moment frames, Journal of Building Engineering 65 (2023) 105629. https://doi.org/10.1016/j.jobe.2022.105629.

[12] Z.-K. Huang, K. Pitilakis, S. Argyroudis, G. Tsinidis, D.-M. Zhang, Selection of optimal intensity measures for fragility assessment of circular tunnels in soft soil deposits, Soil Dynamics and Earthquake Engineering 145 (2021) 106724. https://doi.org/10.1016/j.soildyn.2021.106724.

[13] D.-D. Nguyen, T.-H. Lee, V.-T. Phan, Optimal Earthquake Intensity Measures for Probabilistic Seismic Demand Models of Base-Isolated Nuclear Power Plant Structures, Energies 14 (2021) 5163. https://doi.org/10.3390/en14165163.

[14] D.-D. Nguyen, B. Thusa, M.S. Azad, V.-L. Tran, T.-H. Lee, Optimal earthquake intensity measures for probabilistic seismic demand models of ARP1400 reactor containment building, Nuclear Engineering and Technology 53 (2021) 4179–4188. https://doi.org/10.1016/j.net.2021.06.034.

[15] C. Li, C. Zhai, S. Kunnath, D. Ji, Methodology for selection of the most damaging ground motions for nuclear power plant structures, Soil Dynamics and Earthquake Engineering 116 (2019) 345–357. https://doi.org/10.1016/j.soildyn.2018.09.039.

[16] Nilesh Shome C. Allin Cornell, Probabilistic Seismic Demand Analysis of Nonlinear Structures. (1999).

[17] M. Dolšek, N. Fazarinc (UL), P. Bazzuro, N. Sipcic, P. A. Garcia (IUSS), G. Triantafyllou (IUSS, EDF), I. Zentner (EDF), A. Gerontati, D. Vamvatsikos, Metis Project Deliverable D6.3 "Damage/failure relevant ground motion intensity measures, record selection/generation and site response analysis schemes".

[18] Shome, N., Cornell, C. A., Bazzuro, P., & Carballo, J. E., Earthquakes, records, and nonlinear responses (1998) 469–500.

[19] D. Vamvatsikos, C.A. Cornell, Incremental dynamic analysis, Earthq Engng Struct Dyn 31 (2002) 491–514. https://doi.org/10.1002/eqe.141.

[20] Kramer, S.L. and Stewart, J.P., Geotechnical earthquake engineering (2024).

[21] EPRI, A criterion for determining exceedance of the operating basis earthquake (1988).

[22] Thun, J., Roehm, L. H., Scott, G. A., & Wilson, J. A., Earthquake ground motions for design and analysis of dams (1988) 463–481.

[23] G.W. Housner, Spectrum intensities of Strong-Motion earthquakes (1952) 20–36.

[24] G. W. Housner, Spectrum Intensities of Strong-Motion Earthquakes (1952).
[25] A. Arias, A measure of earthquake intensity. Seismic Design for Nuclear Plants (1970).
[26] P. Anbazhagan, M. Neaz Sheikh, K. Bajaj, P.J. Mariya Dayana, H. Madhura, G.R. Reddy, Empirical models for the prediction of ground motion duration for intraplate earthquakes, J Seismol 21 (2017) 1001–1021. https://doi.org/10.1007/s10950-017-9648-2.
[27] V.V.B. CHIA-MING UANG, Evaluation of seismic energy in structures (1990).
[28] Mackie, Kevin, and Božidar Stojadinović, Probabilistic seismic demand model for California highway bridge (2001) 468–481.
[29] E. Bojórquez, I. Iervolino, Spectral shape proxies and nonlinear structural response, Soil Dynamics and Earthquake Engineering 31 (2011) 996–1008. https://doi.org/10.1016/j.soildyn.2011.03.006.
[30] K. Kostinakis, A. Athanatopoulou, K. Morfidis, Correlation between ground motion intensity measures and seismic damage of 3D R/C buildings, Engineering Structures 82 (2015) 151–167. https://doi.org/10.1016/j.engstruct.2014.10.035.
[31] K. Porter, A Beginner's Guide to Earthquake Fragility Vulnerability and Risk.
[32] N. Shome, Probabilistic Seismic Demand Analysis of Nonlinear Structures. (1999).
[33] Scozzese, F., Tubaldi, E. and Dall'Asta, A., Assessment of the effectiveness of Multiple-Stripe Analysis by using a stochastic earthquake input model. Bulletin of Earthquake Engineering pp.3167-3203.
[34] G.G. Tekeste, A.A. Correia, A.G. Costa, Bayesian updating of seismic fragility curves through experimental tests, Bull Earthquake Eng 21 (2023) 1943–1976. https://doi.org/10.1007/s10518-022-01589-4.
[35] I. Zentner, M. Gündel, N. Bonfils, Fragility analysis methods: Review of existing approaches and application, Nuclear Engineering and Design 323 (2017) 245–258. https://doi.org/10.1016/j.nucengdes.2016.12.021.
[36] Shinozuka, M, Feng, Lee, J, a. Naganuma, T, Statistical Analysis of Fragility Curves.
[37] H. Akaike, Information Theory and an Extension of the Maximum Likelihood Principle.
[38] J.A. Hanley, B.J. McNeil, The meaning and use of the area under a receiver operating characteristic (ROC) curve, Radiology 143 (1982) 29–36. https://doi.org/10.1148/radiology.143.1.7063747.
[39] A. Stocchi, B. Richard, Sensitivity of engineering demand parameters as a function of structural typology and assessment method, Nuclear Engineering and Design 343 (2019) 151–165. https://doi.org/10.1016/j.nucengdes.2019.01.006.
[40] Andrew Whittaker, Gregory Deierlein, John Hooper, Andrew Merovich, Engineering demand parameters for structural framing systems, Applied Technology Council, 2004.
[41] N. Zavala, E. Bojórquez, M. Barraza, J. Bojórquez, A. Villela, J. Campos, J. Torres, R. Sánchez, J. Carvajal, Vector-Valued Intensity Measures Based on Spectral Shape to Predict Seismic Fragility Surfaces in Reinforced Concrete Buildings, Buildings 13 (2023) 137. https://doi.org/10.3390/buildings13010137.
[42] P. Gehl, D.M. Seyedi, J. Douglas, Vector-valued fragility functions for seismic risk evaluation, Bull Earthquake Eng 11 (2013) 365–384. https://doi.org/10.1007/s10518-012-9402-7.
[43] Y. Shen, M. Hesham El Naggar, D.-M. Zhang, Z.-K. Huang, X. Du, Scalar- and vector-valued seismic fragility assessment of segmental shield tunnel lining in liquefiable soil deposits, Tunnelling and Underground Space Technology 155 (2025) 106171. https://doi.org/10.1016/j.tust.2024.106171.
[44] T.H. Sei'ichiro Fukushima, Seismic risk analysis utilizing the PGA and PGV simultaneously as ground motion measures (2009).
[45] M. Yakhchalian, A. Nicknam, G.G. Amiri, Optimal vector-valued intensity measure for seismic collapse assessment of structures, Earthq. Eng. Eng. Vib. 14 (2015) 37–54. https://doi.org/10.1007/s11803-015-0005-6.
[46] Vamvatsikos, D., & Cornell, C. A., Developing efficient scalar and vector intensity measures for IDA (2005).
[47] M. Alembagheri, 2018. Investigating Efficiency of Vector-Valued Intensity Measures in Seismic Demand Assessment of Concrete Dams. Advances in Civil Engineering 2018, 5675032. https://doi.org/10.1155/2018/5675032.
[48] Baker, Jack W., and C. Allin Cornell., A vector-valued ground motion intensity measure consisting of spectral acceleration and epsilon (2005).
[49] V. Bizzarri, Methodology to derive vector-based fragility functions I theoretical aspects - M18.